https://doi.org/10.1016/j.rser.2021.111771

Rechargeable Zn-air Batteries: Recent Trends and Future Perspectives

Kee Wah Leong[b], Yifei Wang[b], Meng Ni[c], Wending Pan[b], Shijing Luo[b], Dennis Y.C. Leung*[a]

[a] Prof. D.Y.C. Leung
Department of Mechanical Engineering
The University of Hong Kong
Pokfulam Road, Hong Kong
E-mail: ycleung@hku.hk
Tel: (852) 3917 7911

[b] K.W. Leong, Dr. Y. Wang, Dr. W. Pan, S. Luo
Department of Mechanical Engineering
The University of Hong Kong
Pokfulam Road, Hong Kong
Email: sl2751@connect.hku.hk, wang1fei@connect.hku.hk, wdpan@connect.hku.hk, luosj@connect.hku.hk

[c] Prof. Meng Ni
Department of Building and Real Estate
The Hong Kong Polytechnic University
11 Yuk Choi Rd, Hung Hom, Hong Kong
Email: meng.ni@polyu.edu.hk

Highlights

- Recent literature results of Zn-air batteries are critically assessed
- Current obstacles of alkaline-based and neutral Zn-air batteries are summarized
- Promising advancements in the anode, electrolyte, and oxygen catalyst are discussed
- Novel trends in solid-state and hybrid Zn batteries are highlighted
- Future perspectives are provided to guide systematic research contributions

Abstract

Currently a hot research topic, rechargeable zinc-air batteries are considered one of the most promising post lithium-ion battery technologies for utility-scale energy storage, electric vehicles, and other consumer electronics. Nevertheless, despite a high energy density, low cost, and material abundance, the development of alkaline-based Zn-air batteries has been hampered by parasitic reactions at the Zn anode and sluggish oxygen redox kinetics. This article will review the current status of Zn-air batteries, discuss recent development trends including neutral and hybrid Zn-air batteries, and highlight future research needs. Specifically, an analysis of the latest publications will show that, through redesigning the anode, introducing alternative electrolytes, and engineering high-performing bifunctional oxygen catalysts, researchers have successfully prolonged the battery reversibility to a few thousand cycles and reached unprecedented energy efficiencies over 70%. Although unsolved obstacles remain, these strategies have opened up interesting possibilities in the advancement of rechargeable Zn-air batteries, creating promising prospects for the energy and electronics industries.
Word count: 9640

Keywords

bifunctional oxygen catalyst, electrolyte, hybrid Zn battery, quasi-neutral electrolyte, quasi-solid-state battery, zinc-air battery

Abbreviations

β-CD: Beta-cyclodextrin
CNT: Carbon nanotubes
CSD: Chemical solution deposition
CVD: Chemical vapor deposition
DEMATfO: Diethylmethylammonium trifluoromethanesulfonate
DMSO: Dimethyl sulfoxide
EDTA: Ethylenediaminetetraacetic acid
EV: Electric vehicle
GN: Graphene nanosheet

GO: Graphene oxide

HCS: Hollow carbon nanospheres

HER: Hydrogen Evolution Reaction

IoT: Internet of Things

KI: Potassium iodide

KOH: Potassium hydroxide

MOF: Metal organic framework

NCF: Nitrogen-doped carbon foam

OCV: Open circuit voltage

OER: Oxygen evolution reaction

ORR: Oxygen reduction reaction

OTf: Trifluoromethanesulfonate

P127: Pluronic F-127

PAA: Polyacrylic acid

PAM: Polyacrylamide

PANa: Sodium polyacrylate

PANI: Polyaniline

PEG: Polyethylene glycol

PPD: Peak power density

PUS: Polyurethane sponges

PVA: Polyvinyl alcohol

rGO: Reduced graphene oxide

SEI: Solid electrolyte interface

TEAOH: Tetraethylammonium hydroxide

TFSI: Bis(trifluoromethanesulfonyl)imide)

VACNT: Vertically aligned carbon nanotube array

ZIF: Zeolitic imidazolate framework

1. Introduction

The growing integration of renewable energy systems has driven a strong interest in energy storage solutions due to the intermittent nature of renewable energy sources. Apart from grid-scale utilities, the increasing consumer adoption of EVs and the ubiquity of IoT sensors have also accelerated the research and development of rechargeable batteries in this energy-conscious, interconnected society. To date, Li-ion batteries are deemed to be the most mature rechargeable battery technology, and are already widely commercialized in consumer products including EVs, medical devices, and other portable electronics. However, due to the high cost, unsatisfactory energy density, and potential toxicity of Li-ion batteries, researchers have begun searching for other alternatives.

In particular, Zn-air batteries have emerged as a promising candidate. Zn metal is a more earth-abundant, low-cost, and environmentally-friendly alternative to Li metal. Deriving energy from Zn and the ample oxygen supply in ambient air, Zn-air batteries are a much more sustainable option than Li-ion batteries. Moreover, the air-breathing cathode makes Zn-air batteries significantly more compact than conventional batteries, contributing to their remarkable theoretical energy densities of 1218 Wh kg^{-1} (gravimetric) and 6136 Wh L^{-1} (volumetric) [1]. In fact, primary Zn-air batteries have already been introduced to the market in the nineteenth century as a power source for hearing aids and pagers, with a practical energy density of 200-500 Wh kg^{-1} [2]. As for rechargeable applications, Zn has a low activity which makes it relatively stable in aqueous electrolytes, offering promise for long-term cyclic operation [3]. They were even proposed as the most suitable energy source for electric vehicles long before the dominance of Li-ion batteries [4]. Nonetheless, long-standing bottlenecks have hindered their development and commercialization. The performance of rechargeable Zn-air batteries is largely limited by the inefficient oxygen reaction kinetics at the air cathode, while their poor cycle stability results from anode degradation and deformation in the conventional alkaline electrolyte. Only in recent years have Zn-air batteries gained renewed interest, mainly due to advances in material science and nanotechnology [5]. In the last decade, researchers have made substantial progress and achieved exciting breakthroughs by optimizing the anode structure, applying additives, exploring alternative electrolytes, engineering oxygen catalysts, and integrating Zn-ion reactions, as summarized in Figure 1, driving Zn-air batteries closer towards the goal of widespread adoption.

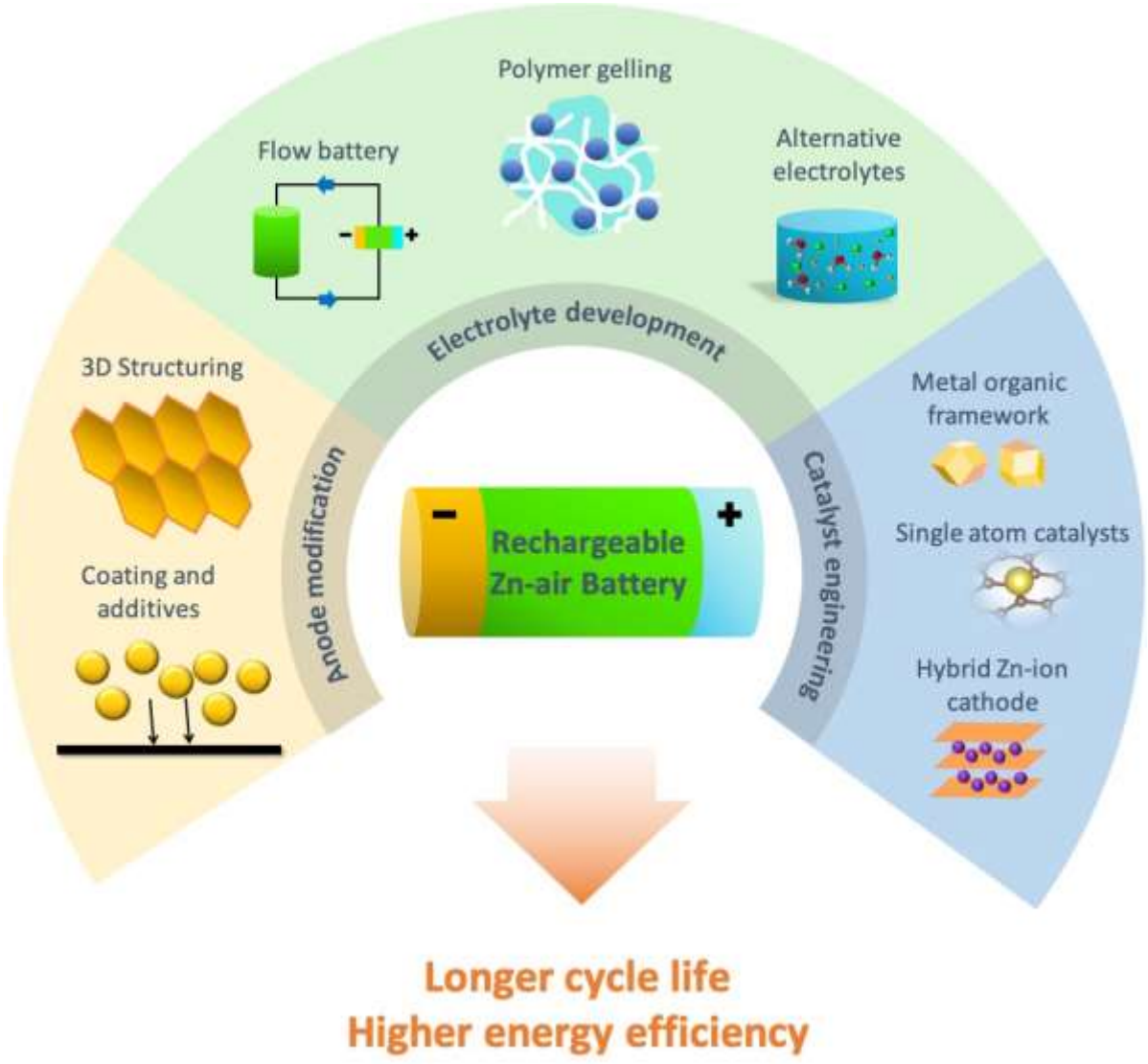

Figure 1 – Schematic summary of recent advancements in rechargeable Zn-air batteries, enabling longer cycle life and higher energy efficiency

There are already numerous review articles on rechargeable Zn-air batteries [6-10], but due to their rapid development and the significant increase in recent research efforts, many new breakthroughs have been made, including novel trends in quasi-solid-state batteries, neutral electrolytes, and hybrid Zn systems. Thus, a timely review of the most recent advances in Zn-air batteries is necessary to provide updated perspectives and to guide future research. Moreover, the most recent review articles on Zn-air batteries only focus on a specific part of the battery—most commonly

the material design of bifunctional oxygen catalysts—without providing a holistic overview of the combined interactions of various components [11-15]. Therefore, in this work, a balanced review of all major components of the Zn-air battery will be presented, specifically focusing on research literatures published in the last five years. First, the working principle and current obstacles of the conventional alkaline-based Zn-air battery will be introduced. Then, the recent advancements in the anode, electrolyte, and oxygen catalyst will be discussed, where the novel classes of Zn-air batteries including quasi-solid-state, neutral, and hybrid systems will be highlighted. The currently achievable battery performances will be compared, and the remaining challenges will be presented. Finally, we will suggest promising paths for further investigation, in the hopes of inspiring more systematic research in Zn-air batteries and closing the gap towards widespread commercialization.

2. Current Status and Obstacles

Currently, several companies have already started deploying Zn-air batteries for utility scale energy storage, including NantEnergy, who installed 3,000 systems in nine countries at a manufacturing cost as low as US$100 per kWh in 2019 [16]. Rechargeable Zn-air batteries are considered one of the most economically feasible battery solutions for grid-scale applications [17]. However, their practical adoption is still in early-stage and limited. Moreover, the currently achievable battery lifetime in practical conditions is only around 150 cycles, and the round-trip energy efficiency is typically less than 60%, which is far from the realistic operational requirements of EVs [18].

One of the most critical obstacles impacting the battery's performance is the deterioration of the Zn anode caused by water-induced parasitic reactions in the electrolyte. A Zn-air battery is typically composed of a Zn anode, an alkaline electrolyte such as KOH, an electrically insulating separator to regulate ion transport, and an air cathode. Despite the high conductivity, low cost, and fast electrochemical kinetics of the alkaline electrolyte, it provides an aggressive chemical environment for the zinc electrode. This section will focus on the current obstacles faced by the traditional alkaline-based system, which is the basis of most publications of Zn-air batteries reported to date. The more recent developments of neutral and hybrid Zn-air batteries and their corresponding challenges will be discussed in Section 3.2.3 and Section 3.4 respectively.

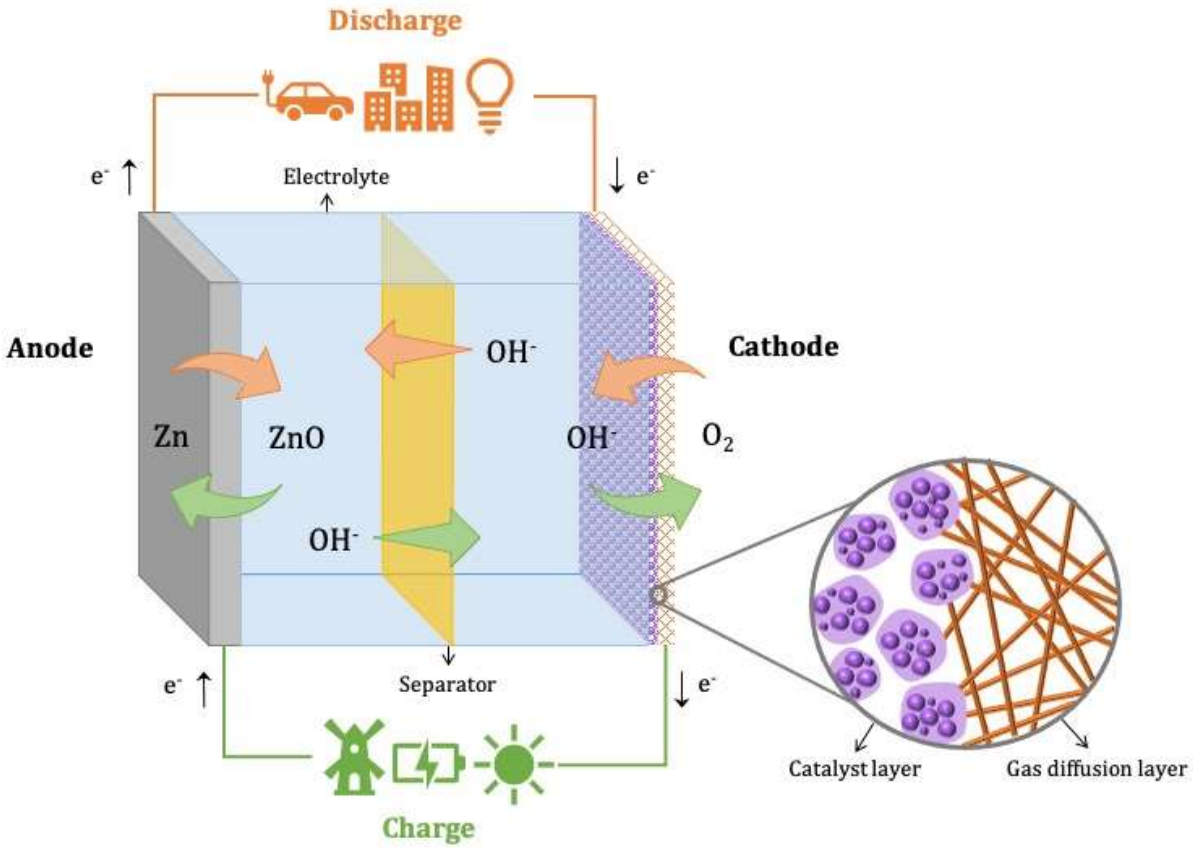

Figure 2 – Schematic representation of a rechargeable Zn-air battery configuration

Figure 2 illustrates the main configuration and working principle of a typical alkaline-based rechargeable Zn-air battery. When a Zn-air battery undergoes discharge, zincate ions ($Zn(OH)_4^{2-}$) are formed in the alkaline electrolyte via the zinc oxidation reaction, where hydroxyl ions (OH^-) are generated via the oxygen reduction reaction (ORR), as described in Equations 1-2a. When $Zn(OH)_4^{2-}$ deposition exceeds the saturation limit, it would further decompose into insoluble ZnO and deposit onto the anode surface (Equation 2b). However, the passivation layer of ZnO would become increasingly compact after repeated cycles, gradually raising the internal resistance and reducing the electrical conductivity of the anode. Eventually, surface passivation could completely block ionic access, thereby adversely affecting Zn utilization and reversibility [19].

Upon electrochemical recharge, ZnO will be reduced back to Zn, and oxygen evolution reaction (OER) will take place at the cathode (Backward reaction of Equation 3). Yet, because of the non-uniform distribution of current densities, the Zn deposition is often uneven, which would densify certain regions of the anode and lead to significant shape change. Then, Zn accumulation on raised

surface heterogeneities would generate sharp, needle-like protrusions, also known as dendrites. Zn dendrites may fracture from the anode and reduce the battery capacity, or even puncture the separator and create short circuiting [1, 20]. Anode deformation and dendrite formation have detrimental effects on the battery rechargeability, which have attracted many research studies.

Cathode: $O_2 + 2H_2O + 4e^- \leftrightarrow 4OH^-$ (1)

Anode: $Zn + 4OH^- \leftrightarrow Zn(OH)_4^{2-} + 2e^-$ (2a)

$Zn(OH)_4^{2-} \leftrightarrow ZnO + H_2O + 2OH^-$ (2b)

Overall: $2Zn + O_2 \leftrightarrow 2ZnO$ (3)

During battery recharge, hydrogen evolution reaction (HER) is another performance-limiting phenomenon. As shown in Equation 4, HER would compete with the anode for electrons, and lower the energy efficiency of the charging process [21, 22]. Moreover, the HER dictates the corrosion rate of the Zn anode, which is thermodynamically unstable in the alkaline electrolyte. At rest, the Zn-air battery will undergo self-discharge, resulting in a shortened shelf life. Besides, HER mainly takes place at high current density sites, where dendrites are located. As hydrogen generation tends to induce convective electrolyte flow, it would further accelerate anode degradation [1, 23, 24]. Zn anode failure due to passivation, shape change, dendritic growth, and hydrogen evolution in the aqueous alkaline electrolyte is currently one of the most critical factors affecting the cycle lifetime of the Zn-air battery.

$$2H_2O + 2e^- \leftrightarrow 2OH^- + H_2 \quad (4)$$

Current obstacles arising from the interaction of the air cathode and the electrolyte also cannot be overlooked. Since water is consumed in the cathode, the aqueous electrolyte suffers from evaporation over time, increasing the concentration of $Zn(OH)_4^{2-}$ ions and speeding up anode degradation. Or worse, the electrolyte would eventually dry out and end the battery operation. In addition, since the catalyst layer of the cathode must be wetted to facilitate the ORR, it is commonly observed that water vapor would accumulate and diffuse out of the air cathode, causing cathode flooding. This not only speeds up electrolyte evaporation, but also causes mass transport problems and raises the cell overpotential [25, 26]. Although a hydrophobic gas diffusion layer is currently added to the air cathode to suppress cathode flooding (Figure 2), a more integrative design of the electrode is favored. Furthermore, electrolyte reactions with carbon dioxide in the

ambient air would generate insoluble carbonates such as potassium carbonate (K_2CO_3), which could impede oxygen transfer when deposited onto the air cathode, thereby lowering the energy efficiency of the Zn-air battery [27].

More critically, the battery efficiency is plagued by the slow redox pathways at the air cathode. The four-electron oxygen chemistry as shown in Equation 1 is notoriously sluggish due to the strong oxygen bonds, leading to high overpotentials in the ORR/OER. Currently, researchers are dedicating substantial efforts in the development of bifunctional oxygen catalysts to accelerate the oxygen reaction kinetics. However, the latest achievable discharge voltages of Zn-air batteries are still lower than the theoretical voltage of 1.66 V at standard conditions. Meanwhile, a recharge voltage of 2 V or higher is often required to reverse the reactions [1, 28]. This is reflected in the wide discharge-charge voltage gap and the poor round-trip energy efficiencies of many Zn-air batteries reported. Round-trip energy efficiency can be calculated by dividing the discharge voltage by the charge voltage at a given current density, which is another indicator of the ratio of useful energy retrieved by the battery. Apart from narrowing the discharge-charge voltage gap, the insufficient energy efficiency during battery cycling must be raised to promote the practical usage of rechargeable Zn-air batteries.

3. Recent Advancements

3.1 Zinc Anode

Substantial research studies have focused on strengthening the reversibility of the Zn anode to increase the cycle life of the Zn-air battery. By extensively exploring the anode design through anode additives and structural modifications, researchers have successfully mitigated various problems of the Zn anode, including dendrite formation, passivation, hydrogen evolution, and corrosion.

3.1.1 Anode Additives and Surface Modification

The application of anode additives can be classified into inorganic and organic additives through the form of alloying and chemical coating. Due to a higher chemical stability, metals such as bismuth, lead, nickel, and cadmium are able to inhibit the HER [29, 30]. Moreover, with a more positive electrode potential, the metal ions can be reduced first during battery charging, thus forming a conductive platform to support more uniform current distributions for the subsequent

deposition of Zn, thereby suppressing dendrite growth [26]. As a result, researchers have explored the integration of these metals and their oxides into the Zn anode. In particular, bismuth and its oxides have emerged as a popular additive choice due to its high electrical conductivity and thermal stability, and its ability to form a solid electrolyte interface (SEI) on the Zn anode surface to reduce corrosion and passivation while promoting electrolyte access [31, 32]. In a primary Zn-air battery, Jo et. al. recently developed a Zn-Bi alloy which exhibited a high corrosion inhibition efficiency of 91.5% and a discharge capacity retention of 99.5% [30]. In a secondary battery, Aremu et. al. used a Zn anode coated with bismuth oxide, potassium sulfide, and lead (II) oxide additives, achieving dendrite-free cycling with superior capacity and no passivation [33].

Other metallic additives have also been explored, such as aluminium oxide, copper oxide, and titanium oxide, which have all shown performance-enhancing effects on the Zn-air battery by establishing a protective anodic layer to minimize spontaneous side reactions [34-36]. Using atomic layer deposition, Zhang et. al. recently developed ZnO@TiN_xO_y core/shell nanorods as the anode where the TiN_xO_y coating successfully mitigated Zn dissolution, lowered internal resistance, and expedited charge transfer, as demonstrated in Figures 3a-e. The thin TiN_xO_y coating effectively blocked bulkier $Zn(OH)_4^{2-}$ molecules while enabling water and OH^- access to the anode, resulting in a battery with stable discharge capacity of 508 $mAhg^{-1}$ over 7500 cycles [37].

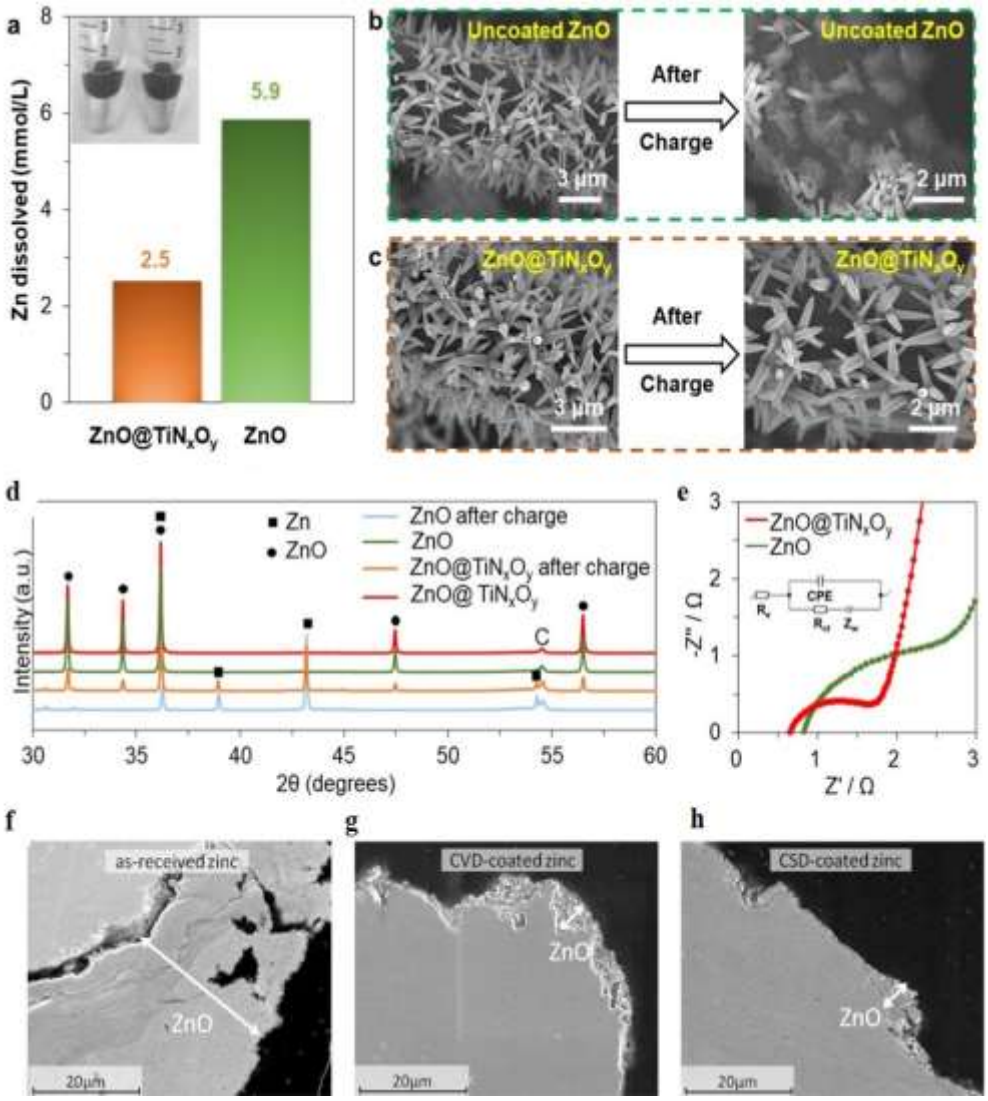

Figure 3 – Effects of anode additives from selected literature (a) Zn dissolution in 4M KOH solution, **(**b)-**(**c) SEM images before and after charge, (d) XRD characterization before and after charge, and (e) EIS results of uncoated ZnO and ZnO@TiN_xO_y nanorod as anodes. Reproduced with permission from Elsevier [37]. (f)-(h) SEM images showing the thickness of passivation layer in, (f) uncoated Zn, (g) CVD-coated Zn, and (h) CSD-coated Zn after discharge. Reproduced with permission from Elsevier [38].

In addition to metal-based additives, silica coatings were also investigated as a safer and more environmentally friendly alternative. Similar to an SEI, silica coatings enable the formation of a $Si(OH)_4$ gel on the anode, which confines $Zn(OH)_4^{2-}$ ions and slows down ZnO precipitation. Schmid et. al. reported a silica-coated Zn anode prepared by chemical vapor deposition (CVD)

and chemical solution deposition (CSD) methods, which suppressed HER by 40% and inhibited passivation, as shown in Figures 3f-h. However, only two cycles were sustained in the Zn-air battery [38]. The long-term effects of silica-based coatings on the extended cycle stability of Zn-air batteries remain unclear.

On the other hand, organic additives such as polyvinyl alcohol (PVA), sodium polyacrylate (PANa), and polyaniline (PANI) hydrogel have proven to inhibit corrosion and self-discharge [39]. Organic coatings generally provide higher controllability, easier fabrication, lower cost, and are more environmentally friendly compared to inorganic anode coatings [40]. Cellulose has also been reported to show superior effects in dendrite reduction compared to lead oxides [41]. Recently, Zhang et. al. introduced a novel ZnO/PVA/β-CD/PEG composite electrode with polymer binders, creating a stable 3D structure to encapsulate the Zn metal and reduce anode deformation, delivering over 80 dendrite-free cycles [42]. However, despite their merits, organic additives could increase battery impedance by acting as insulators and impurities [22]. In general, the use of additives could compromise the specific energy of the battery while adding weight and costs, therefore careful application of the additives and optimization of anode composition are important. The use of inorganic and organic anode additives has shown apparent improvements in mitigating the parasitic anodic reactions by providing an SEI-like protective layer to prevent direct electrolyte access and to immobilize zincate ions. Yet, most reports do not provide sufficient information on the underlying reactions associated with the specific additive material, thus it is difficult to conclude the unique mechanism and effectiveness of each kind of additive relative to one another. Because most of the research attention in recent years is focused on cathode materials instead, the number of studies on anode additives is also lacking. More systematic studies are strongly encouraged to investigate the precise effects of each coating material on anode degradation and battery cycle stability.

3.1.2 Structural alteration

Altering the anode morphology is an effective approach to promote activity and further regulate anode deformation. A structure with excessively large pores could adversely impact the electrode resistance and corrosion rate, but under careful tuning, the increased surface area could facilitate mass transport and electrochemical activity. Lin et. al. observed that a porous Zn anode, electroplated using a frequency of 500 Hz, could produce 60% higher power density with a doubled

specific surface area [43]. Tan et. al. also reported an electroplated Zn on carbon paper that resulted in an excellent battery discharge capacity of 814 $mAhg^{-1}$ at 10 $mAcm^{-2}$. However, the battery could only last for one cycle due to the dissolution of the electroplated Zn [44].

More recently, some researchers have thermally treated the Zn anode to create 3D porous and sponge-like architectures for enhanced reversibility. Compared to conventional powder-based zinc electrodes, the novel 3D structure promotes more uniform current distribution and more effective ionic and electron pathways. It could also confine ZnO deposition within its interior voids, thereby diminishing dendrite growth and improving discharge performance, as illustrated in Figures 4a-b [20]. The compression tolerance of sponge-like electrodes has also opened new doors for battery applications in flexible and stretchable wearable devices. Using electrodeposited Zn nanosheets on nitrogen-doped carbon foams, Pan et. al. presented a sponge-like Zn-air battery with a low discharge-charge voltage gap of 0.657 V at 5 $mA\,cm^{-2}$ and a remarkable power density of 260 $mW\,cm^{-2}$ with strong mechanical endurance properties, as demonstrated in Figures 4c-f [45].

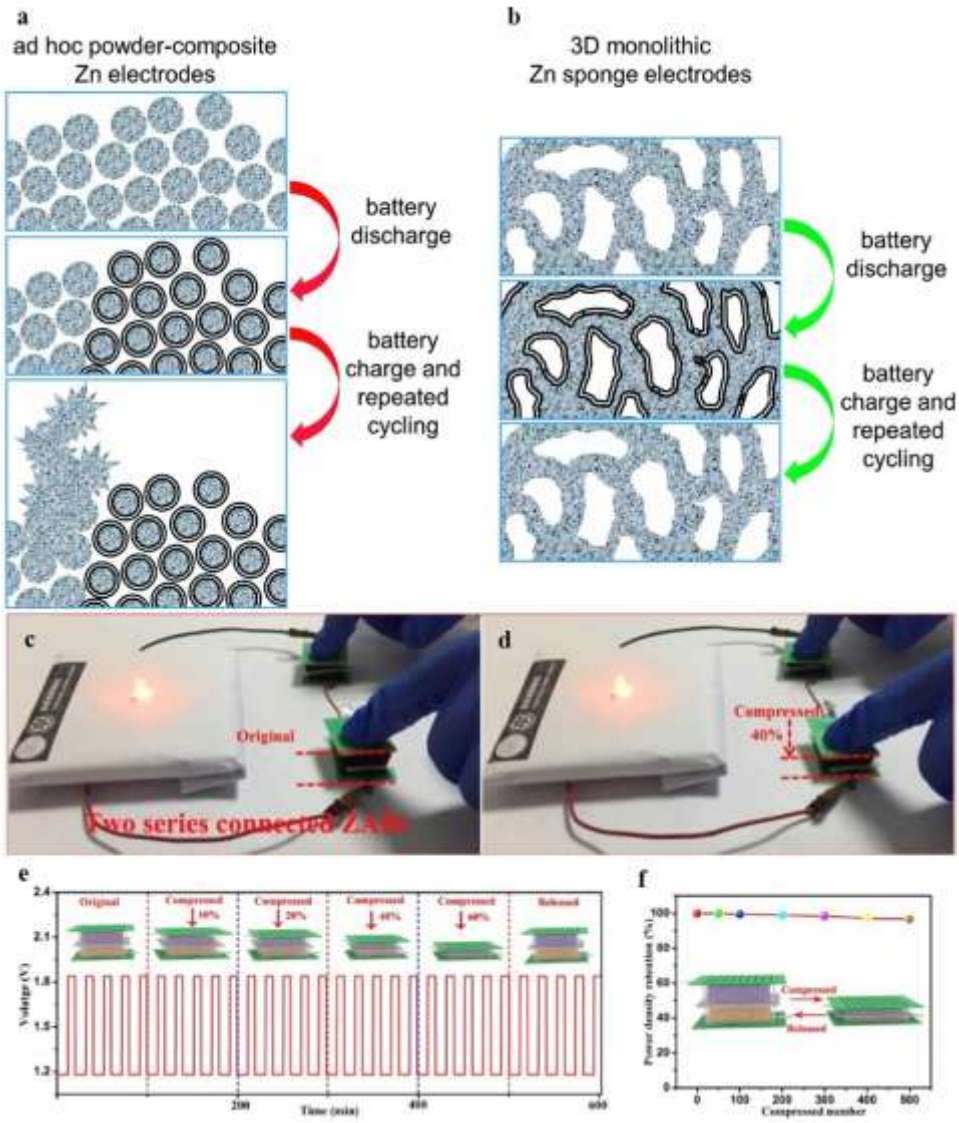

Figure 4 – Schematic diagram of the dissolution-precipitation of ZnO during battery cycling in (a) conventional powder-based Zn anode and (b) the 3D Zn sponge anode. Reproduced with permission from Royal Society of Chemistry [20]. (c)-(d) A light-emitting diode (1.8V) lit up by two squeezable Zn-air batteries under (c) original and (d) 40%-compressed conditions. (e) Galvanostatic discharge-charge curves. (f) Power density retention after various compression cycles. Reproduced with permission from Elsevier [45].

Table 1 presents a selection of recent developments in Zn-air batteries with optimized Zn anodes, as published in literature. Although anode additives and 3D porous structures have proven to be effective solutions to mitigate anode deterioration, many research works have focused on the

measurements of corrosion suppression and HER inhibition without reporting overall battery performance metrics, including cycle stability, peak power density, and energy efficiency. In the cases where galvanostatic discharge-charge operations were tested, the cycle lifetimes of the Zn-air batteries were often unsatisfactory. Thus, in the future, more thorough research studies are required to further promote long-term anode reversibility for practical operations.

Table 1: Selection of Zn-air batteries with optimized anodes published in the last 5 years

Anode Feature	Anode	Discharge capacity ($mAhg^{-1}$)	Discharge-charge voltage gap (V) @ current density[1]	Cycling stability	Ref.
Anode additives	Zn with 3 wt.% Bi_2O_3, 10 wt.% K_2S, 5 wt.% PbO		1.1 (50 $mAcm^{-2}$)	60 cycles, 120 h (50 $mAcm^{-2}$)	[33]
Anode additives	ZnO@ TiN_xO_y nanorods	508		7500 cycles (5 $mAcm^{-2}$)	[37]
Anode additives	SiO_2-coated Zn particles	566		2 cycles (C/20 current rate)	[38]
Anode additives	ZnO/PVA/β-CD /PEG composite			80 cycles (25 $mAcm^{-2}$)	[42]
Anode additives	Zn surface-modified by CuO particles	658	0.782 (50 mAg^{-1})	26.33 h (50 mAg^{-1})	[46]
Anode additives	Zn@C core-shell composite	135		400 cycles (5C current rate)	[47]
Structural alteration	Electroplated Zn on carbon paper	814		1 cycle (10 $mAcm^{-2}$)	[44]
Structural alteration	Electrodeposited Zn nanosheets @ NCF	867 (25 $mAcm^{-2}$)	0.657 (5 $mAcm^{-2}$)	120 cycles (2 $mAcm^{-2}$)	[45]
Structural alteration	Porous Zn with 3D network frame structure	812	0.63 (5 $mAcm^{-2}$)	33 cycles (5 $mAcm^{-2}$)	[48]
Structural alteration	PUS@Zn		0.9 (2 $mAcm^{-2}$)	18 h (2 $mAcm^{-2}$)	[49]

[1] The discharge-charge voltage gap refers to the difference between the charge voltage and the discharge voltage plateaus during galvanostatic cycling. Some of the voltage data are derived from the figures when not reported in text by the authors.

3.2 Electrolyte

Electrolyte development is another crucial focus of recent research efforts in rechargeable Zn-air batteries. In order to increase the anode reversibility and water retention rate, researchers have enhanced the conventional alkaline electrolyte with additives, polymer gel materials, and circulation designs. More novel strategies include developing alternative electrolytes such as quasi-neutral electrolytes and non-aqueous solutions to experiment with more efficient oxygen redox chemistries.

3.2.1 Electrolyte Additives and Flow Battery

Inspired by dendrite inhibition studies in Li-ion batteries, many electrolyte additives such as ethylenediaminetetraacetic acid, tartaric acid, Triton X-100, cetyltrimethylammonium bromide, dimethyl sulfoxide (DMSO), and other organic materials are currently being explored in Zn-air batteries to suppress anode deformation and enhance their rechargeability [50-53]. In particular, sodium dodecyl sulfate (SDS) and other surfactants have become increasingly popular due to their low cost and high safety. Surfactants, which are amphiphilic molecules, contain polymer materials to be adsorbed onto the surface of the anode, acting as a barrier to prevent water contact and ionic access, similar to the mechanism of anode additives. Surfactants also increase the solubility of ZnO molecules and slow down their precipitation, thus reducing anode deformation [22]. Recently, Hosseini et. al. observed a 24% improvement in the specific discharge capacity of a Zn-air battery using SDS, and 30% using nonionic surfactant Pluronic F-127 (P127). Both surfactants retard ZnO dispersion through adsorbing on the Zn anode, however, P127 possesses multiple anchoring groups for stronger surface interactions compared to the single anchoring group in SDS, which resulted in higher cyclic stability [54]. It can be deduced that the different structures of hydrophobic and hydrophilic chains in a surfactant play an essential role in battery performance, which warrants more in-depth studies and experimentation.

Electrolyte additives are commonly coupled with a flow battery, where the electrolyte is circulated through external pumps to remove precipitated carbonates and other by-products. In a Zn-air flow battery, Khezri et. al. used a potassium persulfate additive which diminished Zn corrosion by 56%

[55], while Hosseini et. al. demonstrated a 30% higher discharge capacity and a 16% higher specific energy using ethanol as an eco-friendly additive [56]. More recently, with the use of DMSO, Hosseini et. al. reported excellent passivation inhibition and rechargeability of over 600 cycles in a flow battery, as shown in Figure 5. The application of DMSO not only improves the wettability of the anode surface, thereby promoting the ionic conductivity of the electrolyte, but also forms passive films that increase Zn dissolution while regulating ZnO deposition [57]. Besides, the continuous flow of electrolyte inhibits the saturation of $Zn(OH)_4^{2-}$ ions and also improves OH^- transfer [1].

Model-based studies have also emerged to provide important insights for the rational design and control of the flow battery system. For example, Abbasi et. al. investigated the discharge behavior of Zn-air flow batteries at various discharge currents and electrolyte flow rates, contributing to the validation of current mathematical models. Nonetheless, model-based battery designs are still at an early stage. To develop more accurate models for large-scale practical applications, more accessible experimental data and continuous modelling efforts are needed [58]. More importantly, the power requirements and bulky nature of the electrolyte circulation system still limit its appeal in practical applications, which calls for further system design optimizations.

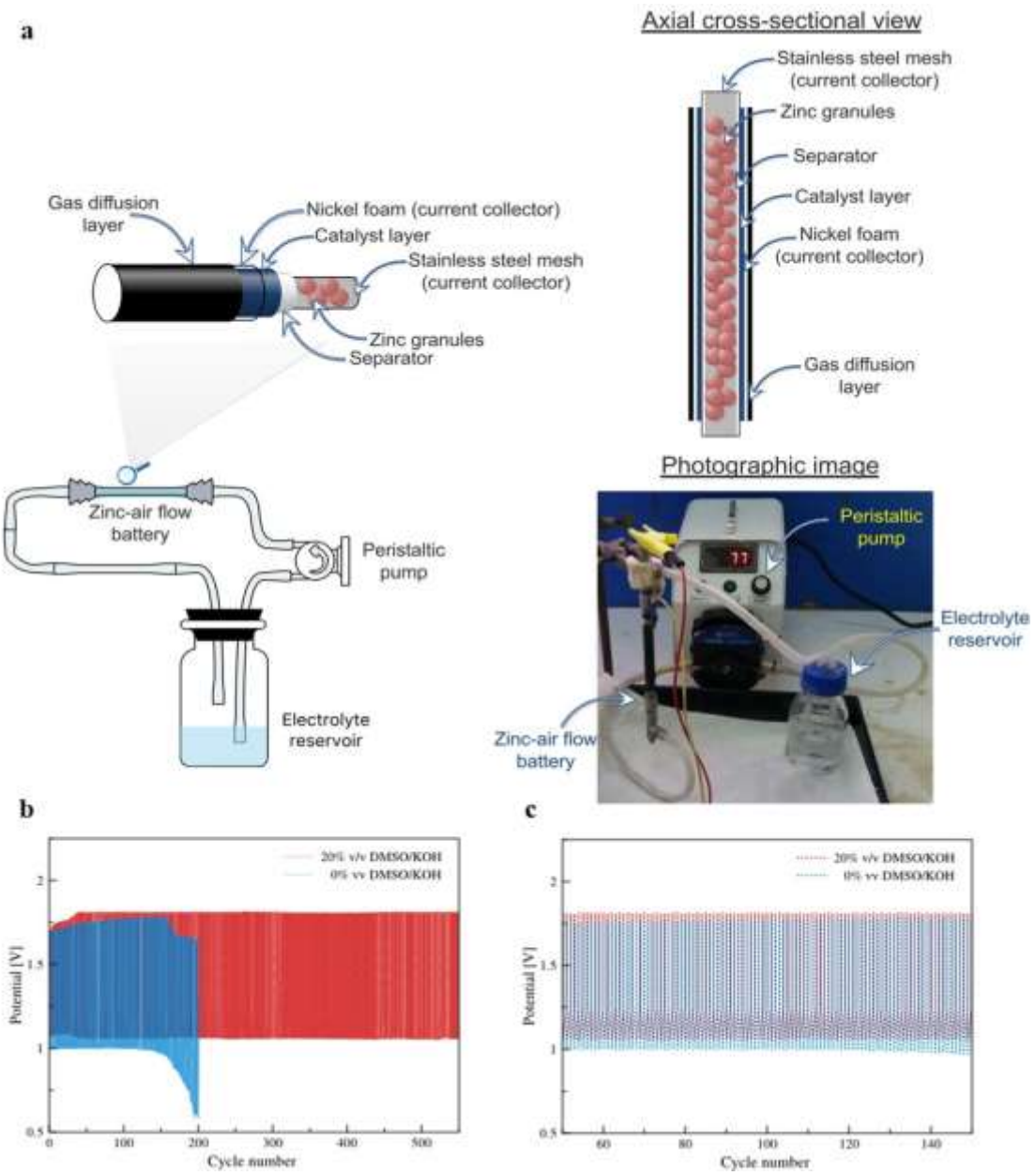

Figure 5 – (a) Schematic configuration and photograph of a Zn-air flow battery; (b)-(c) Galvanostatic discharge-charge profiles of the batteries with and without DMSO additives, discharged at 75 $mAcm^{-2}$ and charged at 25 $mAcm^{-2}$ for 5 mAh: (b) during the 1^{st}-600^{th} cycles, and (c) during the 50^{th}-150^{th} cycles. Reproduced with permission from Springer Nature under the Creative Commons license [57].

3.2.2 Polymer Gel Electrolytes

To prevent Zn anode failure and electrolyte water loss, polymer gel materials have been introduced in alkaline gel hybrid electrolytes, giving rise to quasi-solid-state, flexible Zn-air batteries with improved cycle stability. While PVA-based electrolytes have been extensively investigated, more recent research reveals other polymer gels that surpass its electrochemical performance and water-retention capability, including PANa, polyacrylic acid (PAA), and polyacrylamide (PAM) [59]. Recently, Song et. al. demonstrated a PVA, PAA, and GO co-crosslinked, KI-containing, alkaline electrolyte (KI-PVAA-GO) that enabled flexible Zn-air batteries with a low charging potential of 1.69 V and a discharge potential of 1.24 V at 2 $mAcm^{-2}$, and a robust cycling profile over 200 h with an energy efficiency of 73%. Because gelling often restricts ionic mobility in the electrolyte, highly hydrophilic and alkaline tolerant additives, including KI, quaternary ammonium, and cellulose are often used with polymer gel electrolytes to enhance their ionic conductivity and stability [60]. In a novel PANa-based electrolyte with cellulose additives, Huang et. al. observed the generation of a solid electrolyte interface that facilitated ionic transport and led to stable, dendrite-free battery operation over 800 cycles in 160 hours [61]. Figure 6 illustrates the solid electrolyte interface formation and the practical application of polymer gel electrolytes in solid-state Zn-air batteries for a smart watch. Nonetheless, a further increase in ionic conductivity and mechanical robustness are necessary to extend their operation lives in commercial wearable electronics. Although solid-state batteries are considered much safer than the flammable liquid battery, it is still not completely feasible to use polymer gel electrolytes in practical Zn-air batteries due to the volatility of organic solvents and the low solubility of Zn salts [62].

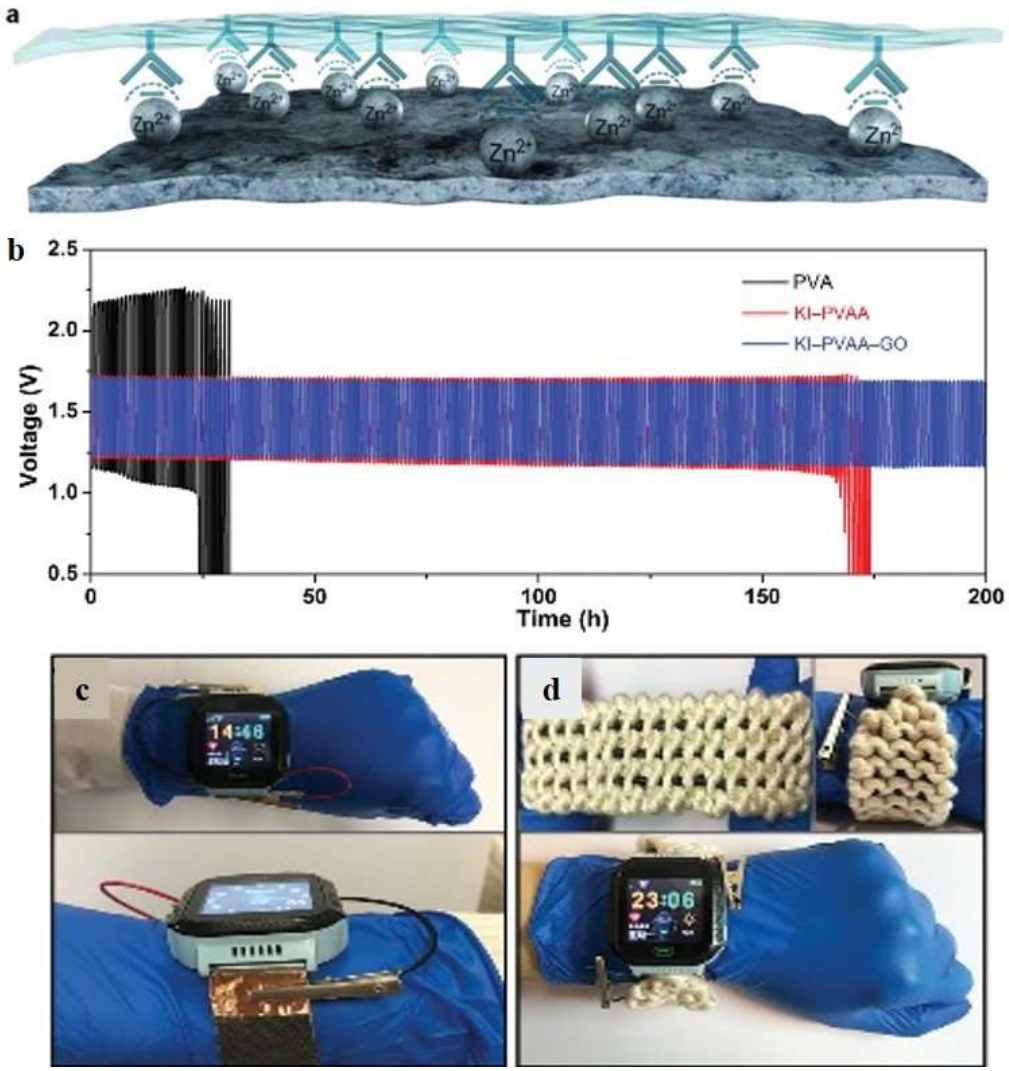

Figure 6 – (a) Schematic illustration of a solid electrolyte interface formed between the Zn anode and PANa electrolyte. Reproduced with permission from John Wiley and Sons [61]. (b) Galvanostatic discharge-charge curves of sandwich-type Zn-air batteries using PVA, PVAA-GO, and KI-PVAA-GO as electrolytes at 2 $mAcm^{-2}$. (c-d) Demonstrations of a flexible Zn-air battery used to power a smart watch in a (c) sandwich-type and (d) cable-type configuration. Reproduced with permission from John Wiley and Sons [60].

3.2.3 Quasi-neutral electrolytes

As a replacement to the traditional alkaline electrolyte, the investigation of chloride- and sulfate-based electrolytes recently enabled a new class of quasi-neutral Zn-air batteries. The most common example is the Leclanché electrolyte, a $ZnCl_2$-NH_4Cl based solution with high ionic conductivity.

The neutral pH of the electrolyte reduces Zn solubility and slows down carbon dioxide absorption, inhibiting dendritic propagation and carbonate formation [63]. The electrodes are also more durable in the milder chemical environment. However, Zn is less active in neutral electrolytes while the oxygen redox kinetics are also slower. In response, Zhang et. al. recently developed a Mn^{2+}-containing Leclanché electrolyte where the addition of the Mn^{2+} salt promotes higher oxygen redox efficiency, delivering dendrite-free cyclic performance over 1350 h with a round-trip energy efficiency of 63% in a Zn-air battery [64]. It is thought that the Zn^{2+} ions would generate zinc complexes that support Zn deposition and mass transfer, thereby suppressing dendrite growth [63]. Most recently, water-in-salt electrolytes have spurred tremendous interest as a type of quasi-neutral electrolytes in between the aqueous and non-aqueous realms. Even though the solvent here is water, the strong concentration of metal salts and the absence of free water molecules could prevent water-induced adverse reactions commonly found in aqueous electrolytes [65]. In 2018, Wang et. al. developed a highly concentrated Zn-ion electrolyte that, when coupled with an air cathode, delivered a battery energy density of 300 W h kg^{-1} and cycling stability over 200 cycles at 50 mA g^{-1} due to the unique solvation structure of Zn^{2+} ions. Characterization results confirmed dendrite-free cycling, while modeling analysis further revealed the suppression of HER [66]. Although water-in-salt electrolytes are more commonly investigated in the context of metal-ion batteries, this pioneering work has demonstrated their compatibility and electrochemical success in a metal-air battery, suggesting the versatility of water-in-salt systems and inspiring new frontiers in the development of neutral Zn-air batteries.

Using an alternative Zn salt with a smaller fluorinated anion, Sun et. al. [67] recently reported a $Zn(OTf)_2$ electrolyte resulting in a zinc peroxide (ZnO_2) chemistry that proceeded through a two-electron ORR rather than the sluggish, conventional four-electron process. The hydrophobic OTf^- ions generated a water-poor and ion-rich Helmholtz layer on the air cathode, facilitating highly reversible redox reactions while preventing water-induced parasitic reactions. Figure 7a illustrates the reversible O_2/ZnO_2 reaction chemistry at the air cathode, which is not possible with hydrophilic anions such as sulfate ions. Compared to a Zn-air battery with an KOH electrolyte, using the $Zn(OTf)_2$ electrolyte also showed a significant inhibition of self-discharge behavior and carbonate formation, as demonstrated in Figures 7b-e. Moreover, surprisingly, only 1 mol kg^{-1} of salt was required here to deliver a discharge capacity of 684 $mAhg^{-1}$ for 320 cycles at 1 $mAcm^{-2}$, suggesting that superconcentrated salt is not always necessary [67], which inspires new possibilities in lower-

cost quasi-neutral electrolytes. However, it is important to note that the two-electron reaction involves intermediates of peroxide that could corrode carbon-based catalysts due to their oxidization tendency [68]. Thus, the catalyst material for the air electrode must be carefully chosen, while a more in-depth understanding of the two-electron oxygen chemistry is crucial.

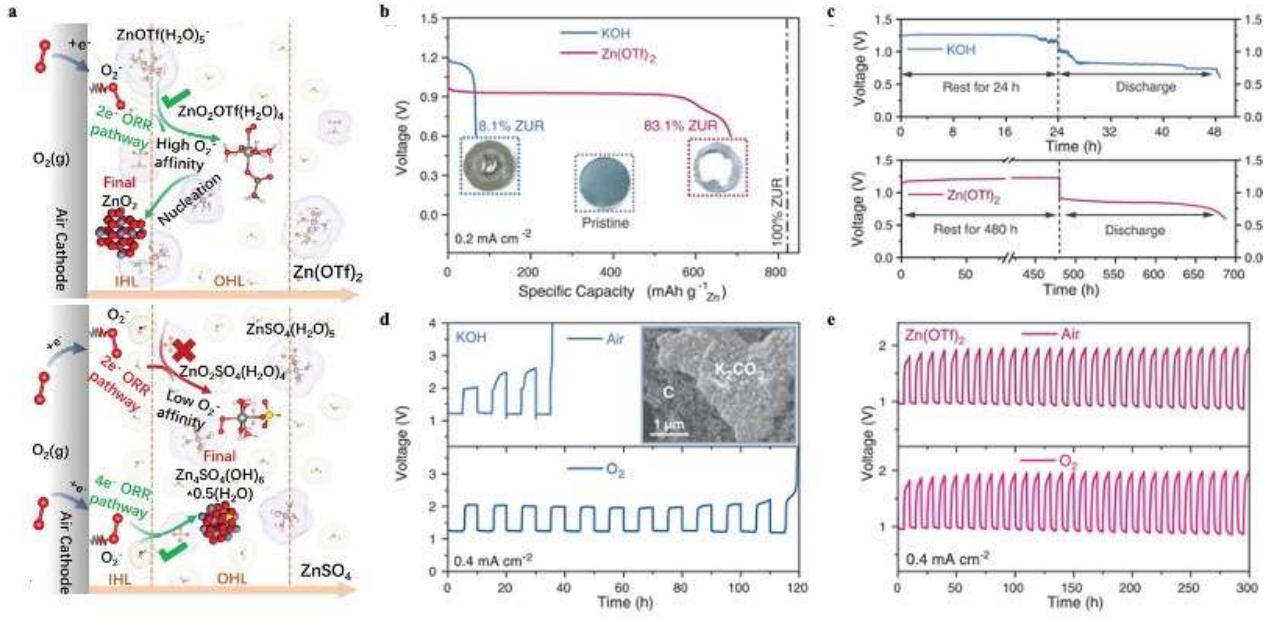

Figure 7 – (a) Schematic illustration of the reaction pathways at the surface of the air cathode in $Zn(OTf)_2$ and $ZnSO_4$ electrolytes. (b-e) Performance comparisons between Zn-air batteries in KOH and $Zn(OTf)_2$ electrolytes: (b) Discharge profiles and zinc utilization rates (ZUR) at 2 $mAcm^{-2}$, (c) Open circuit voltages during 24 h (KOH) and 480 h ($Zn(OTf)_2$) storage, followed by discharge performance, (d-e) Galvanostatic discharge-charge curves at 0.4 $mAcm^{-2}$ under ambient air and O_2 atmosphere, (inset of d) SEM image of K_2CO_3 formation at the air cathode after two cycles in KOH electrolyte. Reproduced with permission from The American Association for the Advancement of Science [67].

Neutral Zn-air batteries circumvent the parasitic reactions associated with the highly corrosive alkaline electrolyte, offering high promise in cycle stability. Nonetheless, research and development are still at an early stage, while publications are still relatively scarce. Neutral electrolytes commonly suffer from pH instability, limited ionic conductivity, and high cost, which must be mitigated to outperform the traditional alkaline-based Zn-air battery. More importantly, the anode reversibility mechanism under quasi-neutral and water-in-salt electrolytes is also not

well understood, which calls for more comprehensive characterizations in order to enable systematic experimentation. Finally, the development of suitable bifunctional oxygen catalysts in neutral media is also essential to improve the oxygen redox kinetics. Despite the promise of neutral Zn-air batteries, there remain important challenges to be solved in order to realize their full potential.

3.2.4 Non-aqueous electrolytes

Non-aqueous electrolytes have been proposed recently to increase battery performance by eliminating water evaporation and parasitic reactions. Using a molten carbonate electrolyte in a Zn-air battery, Liu et. al. reported a high coulombic efficiency of 96.9% and ultralow discharge-charge voltage gap of 0.39 V over 110 cycles. Yet, the cyclic operation was performed under 550 °C to keep the electrolyte in molten state, which is not realistic for room temperature applications [69].

On the other hand, ionic liquid—a molten salt that exists in liquid state at room temperature—has become an attractive option due to their high stability, low-vapor pressure, and non-volatility. In a recent study, Ingale et. al. demonstrated the water retention and dendrite elimination capabilities of the DEMATfO ionic liquid. Without water as a solvent, the ionic liquid enabled a high-performing Zn-air battery with a low discharge-charge voltage gap of 0.6 V over 700 h of stable cycling. However, the power density was unacceptably low due to the low ionic conductivity of the electrolyte [70]. Despite the promising performance of ionic liquids, their lower conductivity, high viscosity, and high cost are the main drawbacks hampering their ability to replace conventional alkaline electrolytes in Zn-air batteries [71, 72].

Table 2 summarizes the recent electrolyte developments for Zn-air batteries enabled by organic and inorganic electrolyte additives, polymer gelling, and novel alternative electrolytes. Despite exciting progress in mitigating anode deformation, water evaporation, and carbonation issues, the average cycle life of Zn-air batteries remains far from satisfactory, as shown in Table 2. Round-trip energy efficiencies of over 70% were achieved in a few recent studies, but the majority still remains low. Compared to conventional alkaline Zn-air batteries, the power density of neutral and non-aqueous Zn-air batteries are significantly restricted due to their poor conductivity. Yet, cyclic stability can be strongly enhanced due to the preclusion of side reactions such as carbonation and corrosion. This is not only reflected in Table 2, but also in a study by Sumboja et. al, who compared

a ph-7 chloride-based Zn-air battery with a conventional alkaline cell. It was observed that the cyclic stability has been extended from 245 cycles to 540 cycles, but the voltage gap doubled and the PPD decreased by eightfold [73]. Although these alternative electrolytes offer enormous potential, their low conductivity calls for more in-depth experimental and model-based development.

Table 2: Selection of Zn-air batteries with enhanced electrolytes published in the last 5 years

Electrolyte feature	Electrolyte	OCV (V)	PPD (mWcm^{-2})	Discharge capacity (mAhg^{-1})	Discharge-charge voltage gap (V) @ current density[1]	Cycling stability @ current density[1]	Round trip efficiency	Ref.
Electrolyte additive + Flow system	Potassium persulfate additive in 7M KOH	1.4		710	0.6 (50 mAcm^{-2})	800 cycles (50 mAcm^{-2})		[55]
Electrolyte additive + Flow system	DMSO in 7M KOH		125	550	0.75 (75 mAcm^{-2})	600 cycles (75 mAcm^{-2})		[57]
Polymer gel	Hydrogel with PANa and cellulose	1.47	210.5	800	0.7 (5 mAcm^{-2})	300 cycles 55 h (5 mAcm^{-2})		[59]
Polymer gel	PVA, PAA, GO alkaline gel with KI additive	1.4	78.6	742	0.45 (2 mAcm^{-2})	200 h (2 mAcm^{-2})	73%	[60]
Polymer gel	PANa hydrogel		88	795	0.68 (2 mAcm^{-2})	800 cycles 160 h (2 mAcm^{-2})	65.5%	[61]
Polymer gel	TEAOH-PVA		74.11	657.9	0.94 (5 mAcm^{-2})	30 h (5 mAcm^{-2})		[74]
Polymer gel	PVA-based gel with silica		123		0.7 (3 mAcm^{-2})	144 cycles, 48 h (3 mAcm^{-2})	63.2%	[75]
Polymer gel	PAM-based alkaline gel	1.32	105	720	0.82 (5 mAcm^{-2})	140 cycles (5 mAcm^{-2})	63.5%	[76]
Polymer gel	PANa alkaline hydrogel	1.45	145		0.75 (2 mAcm^{-2})	400 cycles, 73 h (2 mAcm^{-2})	62%	[77]
Quasi-neutral electrolyte	2M NH_4Cl, 0.2M $ZnCl_2$, 0.02M $MnSO_4$	1.5	7.3	488.6	0.72 (1 mAcm^{-2})	1350 h (1 mAcm^{-2})	63.2%	[64]
Quasi-neutral electrolyte	1 mol kg^{-1} $Zn(OTf)_2$	1.2		684	1 (1 mAcm^{-2})	320 cycles 160 h (1 mAcm^{-2})	55%	[67]
Quasi-neutral electrolyte	1m $Zn(TFSI)_2$ + 20m LiTFSI				1 (50 mAg^{-1})	200 cycles (50 mAg^{-1})		[66]

Quasi-neutral electrolyte	0.1 M NH_4Cl + NH_4OH	1.3	12.8		1.0 (1 $mAcm^{-2}$)	540 cycles, 2160 h (1 $mAcm^{-2}$)	50%	[73]
Non-aqueous electrolyte	Molten $Li_{0.87}Na_{0.63}K_{0.50}CO_3$ with NaOH	1.33			0.39 (25 $mAcm^{-2}$)	110 cycles 50 h (25 $mAcm^{-2}$)	74%	[69]
Non-aqueous electrolyte	DEMATfO ionic liquid		0.045		0.6 (0.05 $mAcm^{-2}$)	700 h (0.05 $mAcm^{-2}$)		[70]
Non-aqueous electrolyte	$ZnCl_2 \cdot 2.33\ H_2O$ molten hydrate	1.4		1000	0.8 (500 mAg^{-1})	100 cycles (500 mAg^{-1})		[78]

[1] The discharge-charge voltage gap refers to the difference between the charge voltage and the discharge voltage plateaus during galvanostatic cycling. Some of the voltage data are derived from the figures when not reported in text by the authors.

3.3 Bifunctional Oxygen Catalyst

Recent research efforts in Zn-air batteries have mainly focused on advancing the material and structural design of bifunctional oxygen catalysts, which can accelerate the electrochemical reaction kinetics at the air cathode while withstanding the alternating cyclic operations. Traditionally, noble metals such as Pt, Ir, and Ru are used in the catalysts, but they are unsustainable and costly. While commercial carbon-supported Pt (Pt/C) exhibits superior ORR activity, its OER performance is poor due to the deposition of an insulating oxide layer [79]. Thus, transition metal-based catalysts have risen as an abundant and low-cost alternative in recent years. Transition metals (Co, Mn, Fe, Ni) and their compounds provide multiple potential oxidation states due to their incompletely filled *d*-orbitals, which promote the electrochemical activity of the catalyst [80]. Transition metal alloys can further improve the catalytic activity of electrodes by a synergistic combination of multiple transition metal species [81, 82]. On the other hand, transition metal oxides can take different lattice or crystal structures, such as monoxide, dioxide, perovskite, and spinel oxides. With abundant oxygen vacancies, perovskites with the general formula of ABO_3 (A: 12-fold oxygen-coordinated metal; B: 6-fold oxygen-coordinated transition metal) and spinel oxides (AB_2O_4) offer enriched active sites and the flexibility for electronic modulation [83, 84]. An example is the widely explored cobalt oxide (Co_3O_4), where Co^{2+} species in tetrahedral sites promotes OER activity and Co^{3+} in octahedral sites helps adsorb oxygen intermediates during ORR [85]. Other transition metal derivatives have also gained research attention in recent years. Compared to transition metal oxides, transition metal nitrides exhibit

higher electron conductivity [86], while transition metal phosphides display stronger OER catalytic activity [87]. Transition metal sulfides also offer fast charge transfer and good adsorption of oxygen intermediates [88].

Nevertheless, transition metal compounds alone are vulnerable under strong electrolytes and harsh redox environments, and prone to particle aggregation. This has inspired the development of metal-carbon composites as bifunctional oxygen catalysts for Zn-air batteries. Metal-carbon composites are typically assembled by anchoring or directly growing metal-based nanoparticles on the functional groups of carbon substrates such as carbon black and porous carbon [89]. Carbon supports could enhance stability, electron conductivity, and the dispersion and utilization of active sites, and also offers flexibility for modulation [82, 90].

Though less common, metal-free carbon-based catalysts are also explored to further decrease costs and environmental impacts by eliminating the use of any metals [91]. In addition, research had begun to utilize biomass as a renewable carbon source for carbon-based catalysts due to environmental and cost concerns on their conventional production from fossil fuels [92]. Recently, rechargeable Zn-air batteries have been developed with the use of table sugar [93] and bamboo leaves [94] as eco-friendly biomass sources for the carbon-based catalyst. Nonetheless, pristine metal-free carbon offers limited active sites and easily corrodes. Therefore, their electronic and morphological structures must be modified to enhance catalytic activity and stability [95].

To this end, structural regulation and defect engineering have been introduced to optimize the activity of bifunctional oxygen catalysts by enriching active sites, accelerating electron transfer, and altering electronic structures. Particularly, promising techniques such as metal organic frameworks and single-atom catalysts are drawing increasing attention in the last few years, leading to prolonged cycle operations and lowered charging potentials in Zn-air batteries. Due to the page limitation, only the latest bifunctional oxygen catalysts that are directly applied in Zn-air batteries have been included in this section.

3.3.1 Structural Engineering

Structural engineering is a popular technique used to enhance the activity of bifunctional oxygen catalysts through morphological manipulation. Similar to porous Zn anodes, the porosity of carbon-based catalysts can be increased to enhance activity and stability. Xiao et. al. recently reported the use of a transition metal oxide $NiCo_2O_4$ embedded into porous carbon as an oxygen

catalyst, exhibiting a narrow discharge-charge voltage gap of 0.73 V and robust stability over 1460 cycles at 10 $mAcm^{-2}$ in a Zn-air battery. $NiCo_2O_4$ offered rich active sites for both ORR and OER, while the porous conductive carbon framework acted as an efficient transport platform for oxygen diffusion and electron transfer, boosting overall battery performance with strong synergistic effects [96].

In metal-carbon composites, nanosized metallic particles are typically anchored onto the carbon substrate to ensure surface contact and expedite charge transfer. However, the synthesis process often causes particle agglomeration. Therefore, 1D and 2D carbon nanostructures have been further introduced to facilitate particle dispersion, in order to improve electron transportation and the accessibility of active sites [97]. Consisting of one-atom-thick layers, graphene possesses excellent electron mobility and a large surface area, which is an ideal platform for particle dispersion [98]. Likewise, carbon nanotubes (CNTs), cylindrical molecules that consist of rolled-up sheets of graphene, also help expedite charge transfer and restrain particle aggregation [99].

In a recent work by Wu et. al., molecularly thin sheets of a NiFeMn trimetallic nitride were stabilized by titanium carbide (Ti_3C_2) sheets, creating an efficient bifunctional oxygen catalyst with robust cyclic performance over 120 h at 20 $mAcm^{-2}$ and a discharge capacity of 627 $mAhg^{-1}$ in a flexible fiber-shaped Zn-air battery [100]. Although it is not the best performing Zn-air battery in recent publications, the synthesis of 2D sheets offers new insights into the structural enhancement of bifunctional oxygen catalysts. Song et. al. also developed a TiC-supported amorphous MnO_x as an oxygen catalyst, which outperformed carbon-supported MnO_x and the state-of-the-art Pt/C-IrO_2 catalyst [101]. These studies suggest new possibilities of corrosion-resistant and highly conductive substrates used to stabilize metal-based catalysts other than carbon-based supports, which tend to corrode and worsen carbonation problems.

The structural modification of bifunctional oxygen catalysts was also further extended by the recent constructions of 3D porous architectures, such as 3D hierarchical Co-N-C nanobrushes [97], and donut-shaped hybrid metal-carbon nanostructures [102]. Using an air electrode of $NiFeO_x$ supported with a 3D, vertically-aligned carbon nanotube array, Yan et. al. achieved an ultralong cycle life of 1500 hours at 5 $mAcm^{-2}$ [103]. Other than metal-carbon composites, 3D structuring has also been applied to pure transition metal compounds and metal-free carbon catalysts, inspiring the fabrication of porous N-doped cobalt pyrite yolk-shell shaped nanospheres (N-CoS_2 YSS) as illustrated in Figures 8a-g [104], and honeycomb-like hierarchical N, O-doped carbon as shown in

Figure 8h. Upon structural manipulation, the N, O-doped carbon catalyst displayed robust stability over 1165 cycles in 388 hours at 10 $mAcm^{-2}$, with a low voltage gap of 0.72 V, and achieved a high peak power density of 261 $mWcm^{-2}$ [105]. Through the rational structural construction of bifunctional oxygen catalysts, the effective surface area can be maximized to accommodate more active sites and enhance diffusion kinetics, resulting in Zn-air batteries with higher energy efficiency.

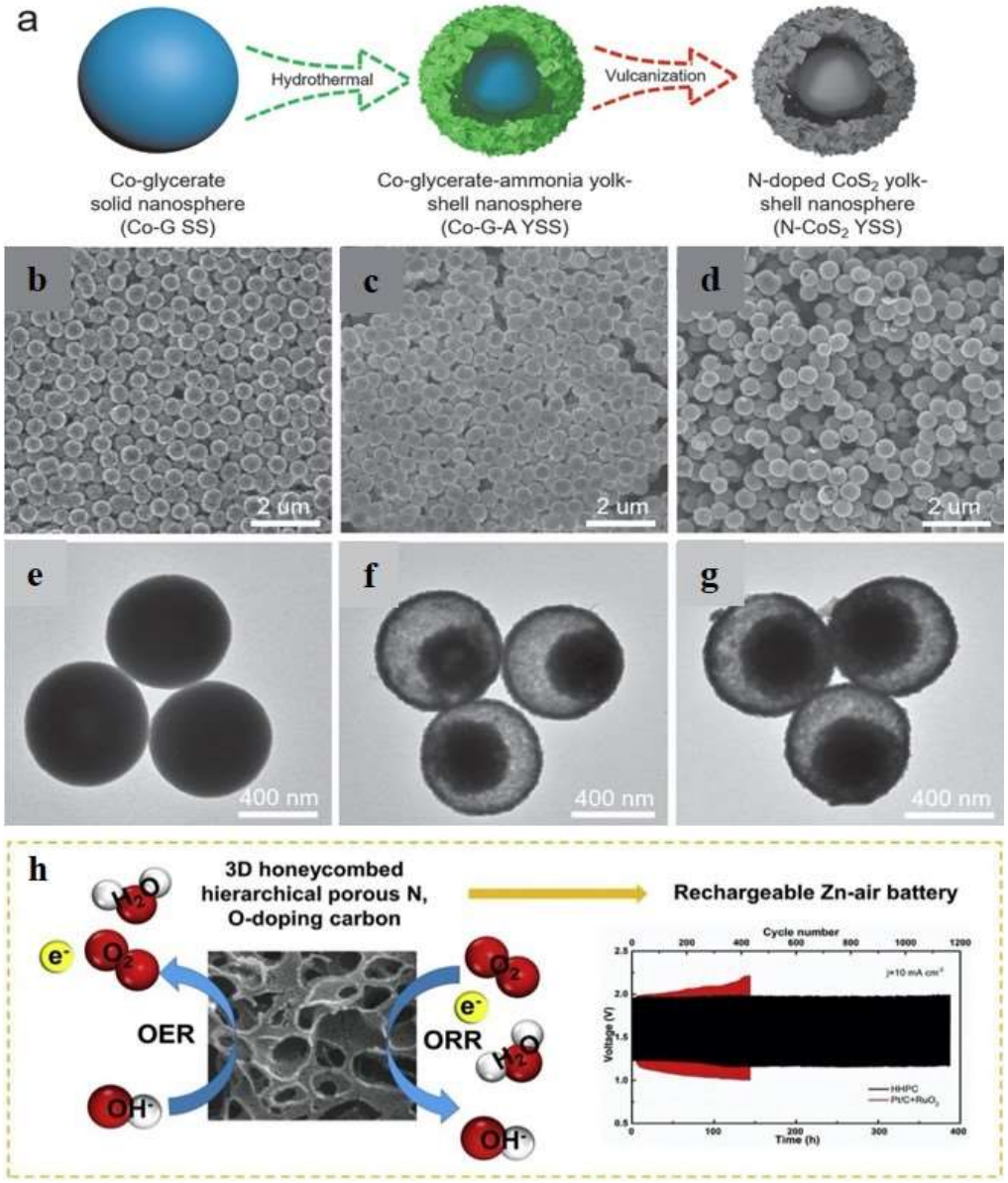

Figure 8 – (a) Schematic illustration of the synthesis of N-CoS_2 YSS. (b,c,d) FESEM, and (e,f,g) TEM images of (b,e) Co-glycerate solid nanosphere Co-G SS, (c-f) Co-glycerate-ammonia yolk-shell nanosphere (Co-G-A YSS), and (d,g) N-CoS_2 YSS. Reproduced with permission from John

Wiley and Sons [104]. (h) Long-term cycling stability at 10 $mAcm^{-2}$ caused by the 3D honeycombed porous structure of N, O-doped carbon. Reproduced with permission from Elsevier [105].

3.3.2 Defect Engineering

Defect engineering promotes the electrochemical activity of catalysts through the introduction of active sites and the regulation of charge distributions. For example, rich edge sites and topological defects in graphene derivatives like graphene oxide (GO) and reduced graphene oxide (rGO) provide intrinsic activity and offer anchoring points for other active metals and heteroatoms [106-108]. Taking advantage of this, Shu et. al. uniformly dispersed cobalt nitride nanoparticles on the surface of rGO, which formed unique worm-shaped holes on the $Co_{5.47}N$@N-rGO catalyst that further exposed active sites, delivering robust battery operation of 2000 cycles over 330 hours. However, its round-trip energy efficiency was only 57%, which urges further research and optimization [109].

Oxygen defects can also enhance electrical conductivity in the catalyst by stimulating the delocalization of electrons. To do so, a common method is surface etching, which includes ammonia surface treatment, plasma etching, and ball-milling [110]. For example, Li et. al. recently created oxygen defects in the atomic layer of cobalt oxides (Co_3O_{4-x}) nanosheets using plasma treatment, delivering superior cyclic performance over 150 hours at 5 $mAcm^{-2}$ and achieving a lower overpotential for OER compared to commercial IrO_2 in a rechargeable Zn-air battery [111].

Heteroatom doping is also a common strategy to introduce defects. The doping of carbon materials is a process that replaces some carbon atoms with heteroatoms such as N, S, or P. These heteroatoms can introduce electron depletion on carbon atoms and optimize valence orbital energy for active sites [84, 107]. Lyu et. al. reported a metal-free N, S co-doped carbon catalyst, where the binary doping generated an asymmetric distribution of the charge and spin density of carbon atoms, leading to remarkable ORR and OER activity [112].

Heteroatom doping is an essential feature in transition metal-based nitrogen-doped carbon materials (M-N-C, M: transition metal), a high-performing class of metal-carbon composites. The synergistic interactions between metals and N-doped carbon promote catalytic activity by altering the electronic structure and facilitating the adsorption and desorption of O_2 and intermediates [97]. Using a MgO-templated carbonization process, Tang et. al. synthesized a Co/N/O tri-doped

graphene catalyst with atomically dispersed Co-N_x-C active sites, delivering superior bifunctional activities with a narrow cycling voltage gap of 0.7 V at 1.0 $mAcm^{-2}$ in a flexible Zn-air battery. However, the battery only operated for 18 cycles over a period of 1 hour, which was insufficient to prove its long-term cycle stability [106].

3.3.3 Metal organic framework (MOF)

To prepare M-N-C hybrids and other functional catalysts including metal alloys and heteroatom-doped carbon, metal-organic framework (MOF)-derived methods have recently emerged as a promising approach due to their low cost, tailorable nature, and potential for high-throughput synthesis. MOF is a novel class of porous crystalline structures consisting of metal ions coordinated to organic ligands. Combining the benefits of both structural and defect engineering, the high surface area and porosity of MOFs can accelerate mass transfer and expose active sites, while heteroatom doping can introduce defects and avoid particle agglomeration during pyrolysis [113, 114].

A common example of MOF is the zeolitic imidazolate framework ZIF-67, which consists of Co^{2+} ions and 2-methylimidazole, and is widely applied in bifunctional Co-N-C catalysts [115]. Figure 9a illustrates a typical template-guided preparation process. Zhou et. al. synthesized a catalyst composed of Co nanoparticles embedded in hollow N-doped carbon tubes (Co@hNCT) through the growth of ZIF-67 nanocrystals. The porous conductive framework expedited electron and ion transfers, while maximizing the utilization of active sites, resulting in a Zn-air battery with a high power density of 149 $mWcm^{-2}$ and stable cycling at 5 $mAcm^{-2}$ over a period of 500 hours, as shown in Figures 9b-d [114]. In fact, a recent study by Xu et. al. reported one of the longest cyclic operations of Zn-air batteries to date—over 3000 hours (9000 cycles) at 5 $mAcm^{-2}$, and a narrow discharge-charge potential gap of 0.76 V, enabled by the development of a MOF-derived Co supported with N-doped CNT/graphene hybrid [116]. MOF-derived bifunctional oxygen catalysts show great promise for the performance enhancement of recent Zn-air batteries, which call for continuous investigation and advancement.

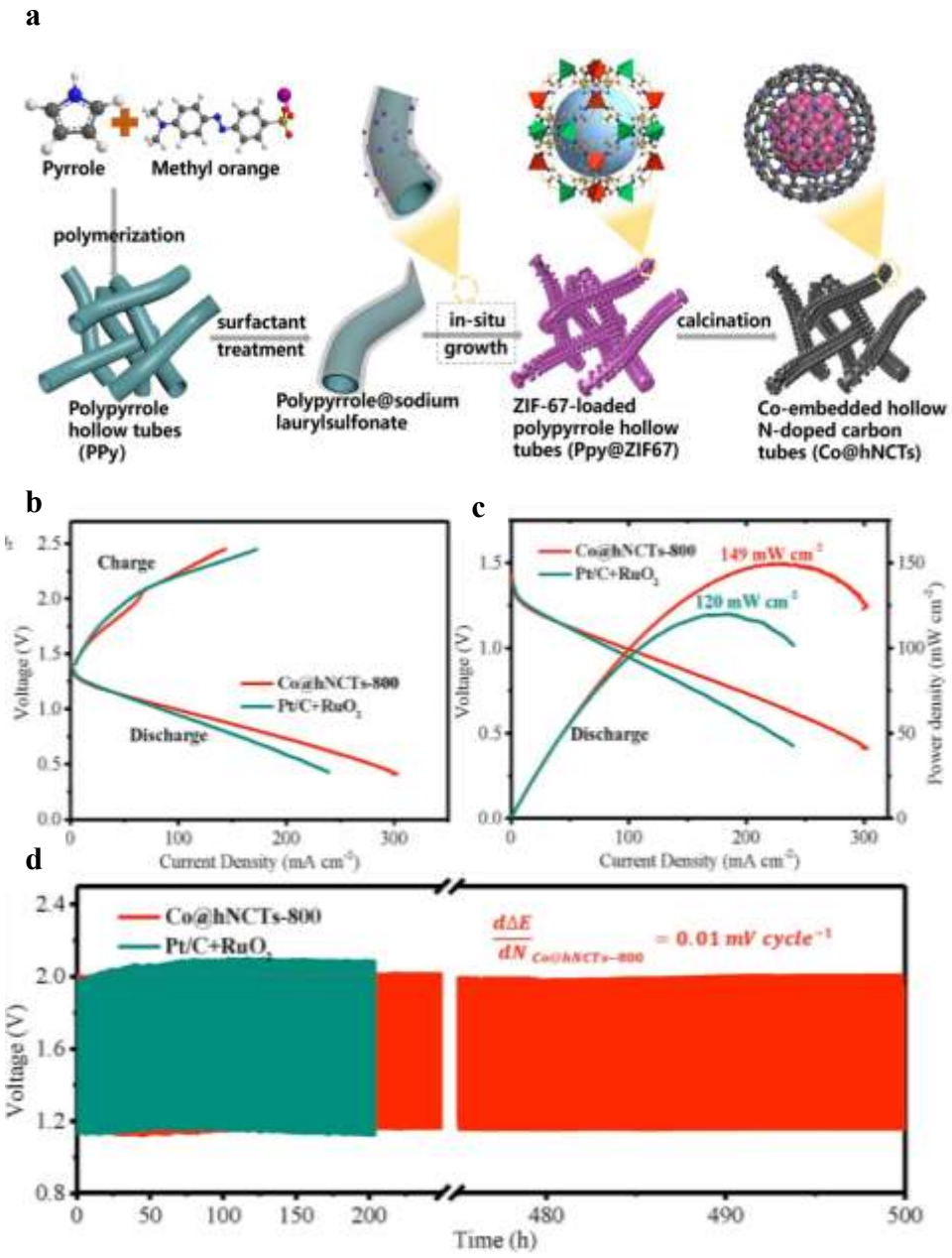

Figure 9 – (a) Schematic illustration of the synthesis of MOF-derived Co@hNCT. (b) Charge and discharge polarization curves, (c) discharge polarization and power density curves, and (d) galvanostatic cycling profile of Zn-air batteries with hollow N-doped carbon tubes as catalyst, compared with commercial Pt/C + RuO_2 at a 5 $mAcm^{-2}$. Reproduced with permission from Elsevier [114].

3.3.4 Single Atomic Engineering

Single atomic engineering is another novel trend in the catalyst field, which involves the dispersion of isolated metal atoms over a host substrate. Figure 10a compares the structures of nanoparticles and single atom catalysts, and shows that every atom in a single atom catalyst can be potentially utilized for catalytic activity. The high atomic utilization in single atom catalysts opens new frontiers in metal-carbon composites as oxygen catalysts [117, 118].

In 2019, Han et. al. fabricated a single-atom Co catalyst anchored on N-doped carbon by tuning the composition of Zn and Co in the bimetallic ZnCo-ZIFs precursors, as shown in the characterization images in Figures 10b-d. Compared to nanoparticles and atomic clusters (Figures 10e-f), single-atom Co catalysts (Figure 10g) exhibited higher bifunctional catalytic activity and reversibility in Zn-air batteries [119]. Sun et. al. further introduced P-O doping in an Fe single-atom site which successfully reduced the reaction overpotential of the Zn-air battery. The resulting battery showed a superior peak power density of 232 $mWcm^{-2}$ and robust cyclic performance over 450 cycles at 25 $mAcm^{-2}$ [120].

Single atomic engineering is a significant breakthrough in catalyst development because of the precise and controlled construction of catalysts in the atomic level. Yet, the low metal loading of current single atom catalysts must be increased in order to maximize the promise of single atom catalysts in practical and scalable assembly of Zn-air batteries. The stabilization of isolated atoms in single atom catalysts with high metal loading is particularly difficult, and current fabrication processes remain relatively inefficient [121]. However, in a recent study, a novel multilayer stabilization method has emerged to enable the construction of high-loading single atom catalysts in N, S, F co-doped graphitized carbons, which offers an exciting opportunity for future development and adaptation [122].

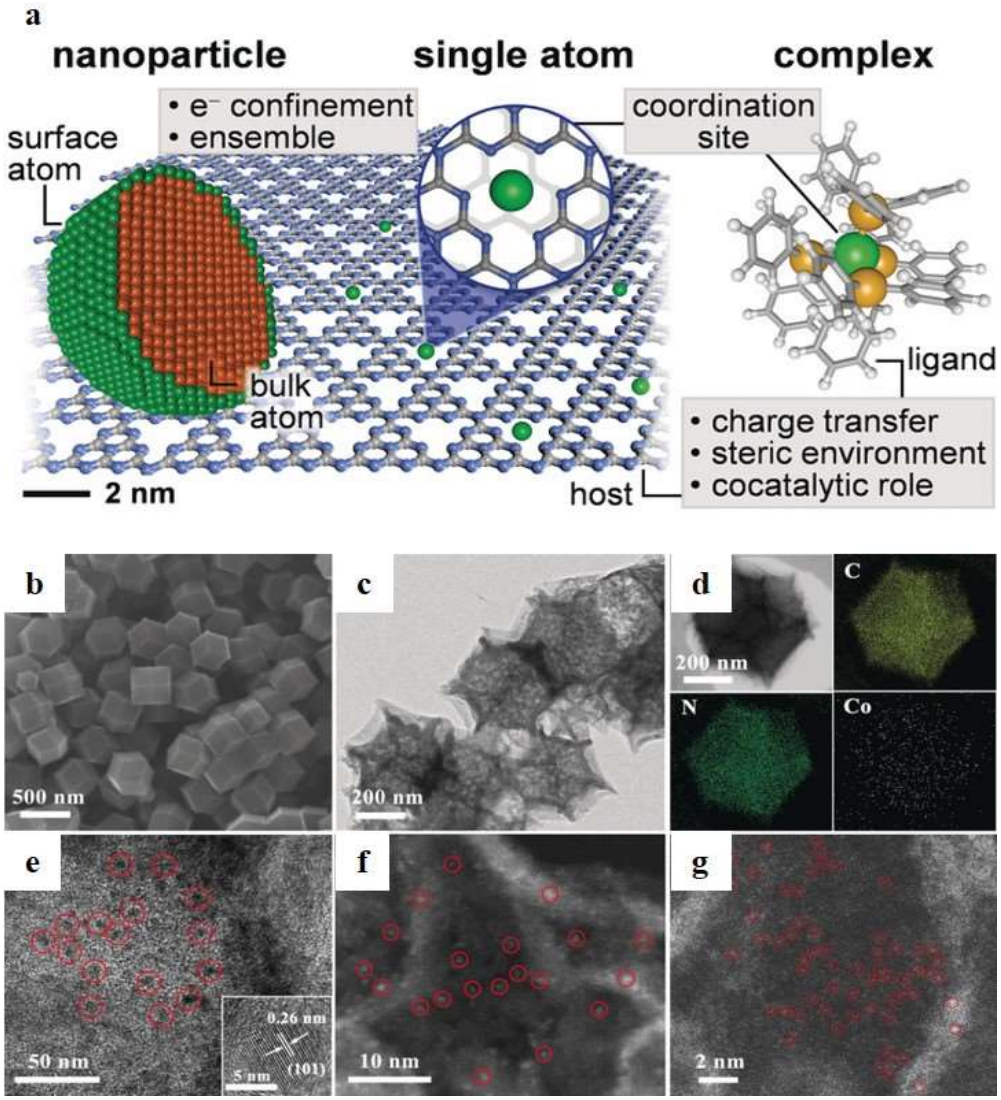

Figure 10 – (a) Comparison of structural features and distinct properties of metal catalysts based on nanoparticles and single atoms. Reproduced with permission from John Wiley and Sons [118]. (b) SEM and (c) TEM images and (d) EDS mapping of cobalt single atoms on N-doped carbon (Co-SAs@NC). (e) TEM image of cobalt nanoparticles on N-doped carbon. (f,g) HAADF-STEM images of (f) cobalt atomic clusters on N-doped carbon and (g) Co-SAs@NC. Reproduced with permission from John Wiley and Sons [119].

Table 3 presents the latest publications on novel catalyst developments optimized by structural regulation, defect engineering, MOF-derived synthesis, and single atomic dispersion, which have led to improved performances in rechargeable Zn-air batteries. With the use of advanced bifunctional oxygen catalyst materials and engineering strategies, superior discharge capacities

could be reached, while narrow discharge-charge voltage gaps over a few thousand cycles have been achieved, creating unprecedented progress in the development of Zn-air battery. Nevertheless, the latest reported round-trip energy efficiencies are still under 70%. To further advance the development of the oxygen catalyst, more in-depth investigations of the material formation processes is necessary to enable their controlled tuning and precise optimization.

Table 3: Recent advances in bifunctional oxygen catalysts for Zn-air batteries in the last 5 years

Cathode modification	Cathode catalyst	OCV (V)	PPD (mW cm^{-2})	Discharge capacity ($mAhg^{-1}$)	Discharge-charge voltage gap (V) @ current density[1]	Cycling stability @ current density[1]	Round trip efficiency	Ref.
Structural engineering	$NiCo_2O_4$ nanowhiskers in porous carbon	1.48	267	767	0.73 (10 $mAcm^{-2}$)	1460 cycles, 487 h (10 $mAcm^{-2}$)	62.2%	[96]
Structural engineering	Molecularly thin sheets of NiFeMnN stabilized by Ti_3C_2	1.50		627	0.68 (20 $mAcm^{-2}$)	120 cycles, 120 h (20 $mAcm^{-2}$)		[100]
Structural engineering	Donut-shaped hybrid of CoP@ P,N-doped carbon matrix		139	730.55	0.94 (30 $mAcm^{-2}$)	350 cycles, 150 h (30 $mAcm^{-2}$)		[102]
Structural engineering	$NiFeO_x$@ VACNT	1.45	194	800	0.87 (5 $mAcm^{-2}$)	4500 cycles, 1500 h (5 $mAcm^{-2}$)		[103]
Structural engineering	Porous N-doped cobalt pyrite yolk-shell nanospheres	1.41	81	744	0.85 (10 $mAcm^{-2}$)	165 h (10 $mAcm^{-2}$)	56%	[104]
Structural engineering	3D honeycomb N, O-doped carbon		261		0.72 (10 $mAcm^{-2}$)	1165 cycles, 388 h (10 $mAcm^{-2}$)		[105]
Structural engineering	Honeycomb-like Co-N_x-C Nanopolyhedron		110		1.03 (10 $mAcm^{-2}$)	100 h (10 $mAcm^{-2}$)		[123]
Structural engineering	$NiCo_2S_4$ urchin-like structure				0.82 (2 $mAcm^{-2}$)	60 cycles (2 $mAcm^{-2}$)	68.8%	[124]
Structural engineering	Mesoporous Ni/NiO Nanosheets on carbon fiber paper	1.47	225	853	0.83 (2 $mAcm^{-2}$)	240 cycles, 120 h (2 $mAcm^{-2}$)	57.1%	[125]
Defect engineering	Co/N/O tri-doped graphene	1.44	152	750	0.7 (1 $mAcm^{-2}$)	18 cycles, 1 h (1 $mAcm^{-2}$)	63%	[106]

Defect engineering	$Co_{5.47}N$@ worm-like structure of porous N-rGO	1.45	121	789	0.77 (1 $mAcm^{-2}$)	2000 cycles, 330 h (1 $mAcm^{-2}$)	56%	[109]
Defect engineering	Oxygen defect Co_3O_{4-x} nanosheets		122	791	0.5 (5 $mAcm^{-2}$)	450 cycles, 150 h (5 $mAcm^{-2}$)		[126]
Defect engineering	N,F-doped carbon	1.33	130		0.85 (20 $mAcm^{-2}$)	49 h (20 $mAcm^{-2}$)	60.9%	[127]
Defect engineering	Co/NC		196	766	0.88 (5 $mAcm^{-2}$)	12 h (5 $mAcm^{-2}$)		[128]
Defect engineering	Fe/Fe_3O_4@N-HCS	1.41	93.6		0.8 (10 $mAcm^{-2}$)	25 cycles, 100 h (10 $mAcm^{-2}$)		[129]
Defect engineering	Spinel $CoIn_2Se_4$ nanosheet	1.37	107	733	0.71 (10 $mAcm^{-2}$)	400 cycles (10 $mAcm^{-2}$)	63.6%	[130]
Defect engineering	Co_xS_y@S,N co-doped mesoporous carbon	1.35	136	777	0.88 (20 $mAcm^{-2}$)	600 cycles, 100 h (20 $mAcm^{-2}$)	62.3%	[131]
Defect engineering	FeNiP/N,P-doped carbon nanosheets	1.51	163	603	0.58 (10 $mAcm^{-2}$)	330 cycles, 110 h (10 $mAcm^{-2}$)	69%	[132]
Defect engineering	$LaCo_{0.8}Ru_{0.2}O_{3-\delta}$ (Ru substitution in LaCoO)	1.28	136	433	0.78 (5 $mAcm^{-2}$)	1440 cycles, 240 h (5 $mAcm^{-2}$)	60%	[133]
Defect engineering	Pd-modulated B-site doped single perovskite	1.5	52	740	0.9 (10 $mAcm^{-2}$)	60 cycles, 60 h (10 $mAcm^{-2}$)		[134]
MOF-derived	HCo@ FeCo/N/C	1.45	125		0.84 (10 $mAcm^{-2}$)	200 h (10 $mAcm^{-2}$)		[135]
MOF-derived	Co@N-CNT	1.45	149	746	0.85 (5 $mAcm^{-2}$)	500 h (5 $mAcm^{-2}$)		[114]
MOF-derived	Co/N-doped CNT/graphene hybrid	1.48	253	801	0.76 (5 $mAcm^{-2}$)	9000 cycles, 3000 h (5 $mAcm^{-2}$)		[116]
MOF-derived	Co_9S_8/GN		186		0.52 (2 $mAcm^{-2}$)	2000 cycles, 147 h (2 $mAcm^{-2}$)		[136]
MOF-derived	CoP/ N,P-doped C	1.4	186		1 (2 $mAcm^{-2}$)	80 h (2 $mAcm^{-2}$)		[137]
MOF-derived	Ni-Co-S/ N, S-doped porous carbon	1.43	137	829	0.73 (10 $mAcm^{-2}$)	180 cycles (10 $mAcm^{-2}$)		[138]
MOF-derived	$Co@SiO_x$ /N-doped carbon framework		138		0.82 (5 $mAcm^{-2}$)	400 h (5 $mAcm^{-2}$)		[139]

MOF-derived	Co/Co_9S_8@CNT	1.44	185		0.75 (5 $mAcm^{-2}$)	50 cycles, 2000 h (5 $mAcm^{-2}$)		[140]
MOF-derived	$Ba_{0.5}Sr_{0.5}Co_{0.8}Fe_{0.2}O_3$ perovskites				0.83 (5 $mAcm^{-2}$)	1800 cycles, 300 h (5 $mAcm^{-2}$)		[141]
MOF-derived	Co-MOF/ $LaCoO_{3-\delta}$ hybrid	1.44	126		0.67 (5 $mAcm^{-2}$)	120 h (5 $mAcm^{-2}$)	66.5%	[142]
MOF-derived	CoO/Co_xP Trimurti Heterostructured Hybrid	1.4	123		0.86 (5 $mAcm^{-2}$)	400 cycles, 202 h (5 $mAcm^{-2}$)		[143]
MOF-derived	Ni_1Co_3@ N-CNTs	1.446	98.2	721.6	0.71 (5 $mAcm^{-2}$)	200 h (5 $mAcm^{-2}$)		[144]
MOF-derived	Ni_3Fe/ Co-N-C	1.39	68		0.75 (10 $mAcm^{-2}$)	65 h (10 $mAcm^{-2}$)	64.3%	[145]
MOF-derived	Co-NCS@nCNT	1.42	90	798	0.89 (5 $mAcm^{-2}$)	480 cycles, 80 h (5 $mAcm^{-2}$)	66.6%	[146]
MOF-derived	Co_3O_4/Co@NC	1.5	124		0.94 (10 $mAcm^{-2}$)	3600 cycles, 600 h (10 $mAcm^{-2}$)		[147]
MOF-derived	N-doped CNT matrix	1.5	220	797	0.8 (5 $mAcm^{-2}$)	4800 cycles, 1600 h (5 $mAcm^{-2}$)		[148]
Single atom catalyst	Co single atoms@NC	1.4			0.7 (1 $mAcm^{-2}$)	17 h (1 $mAcm^{-2}$)		[119]
Single atom catalyst	P−O-doped single atom Fe-N-C	1.41	109		0.77 (10 $mAcm^{-2}$)	20 h (10 $mAcm^{-2}$)	61%	[120]
Single atom catalyst	Single atom FeCo/ N-doped HCS	1.43	86.7	819.6	0.88 (5 $mAcm^{-2}$)	300 cycles, 100 h (5 $mAcm^{-2}$)		[149]
Single atom catalyst	Fe-N_x-HCS	1.42	154	422	1 (10 $mAcm^{-2}$)	58 h (10 $mAcm^{-2}$)		[150]
Single atom catalyst	Co single atoms-Co_3O_4@ N-doped active carbon	1.45	164	721	0.77 (10 $mAcm^{-2}$)	35 h (10 $mAcm^{-2}$)		[151]
Single atom catalyst	Single-atom Co-N_x-C	1.4	78		1.04 (2 $mAcm^{-2}$)	200 cycles 79 h (2 $mAcm^{-2}$)		[152]
Single atom catalyst	Single atom Fe/N-G	1.4	120		0.78 (10 $mAcm^{-2}$)	240 cycles (10 $mAcm^{-2}$)		[153]
Single atom catalyst	Co single atoms@NC	1.41	20.9		0.45 (10 mA cm^{-2})	42 h, 125 cycles (10 mA cm^{-2})		[154]

[1] The discharge-charge voltage gap refers to the difference between the charge voltage and the discharge voltage plateaus during galvanostatic cycling. Some of the voltage data are derived from the figures when not reported in text by the authors.

3.4 Hybrid Zinc Battery

Despite the development of bifunctional oxygen catalysts, the working voltage of zinc-air batteries is still limited to a maximum theoretical value of 1.66 V only. As a result, there has been an increasing number of recent studies on hybrid Zn batteries, which combine the Zn-air reaction with other Zn-ion systems such as Zn-Ni, Zn-Co_3O_4, and Zn-Ag reactions to raise its theoretical potential. These Zn-ion batteries exhibit higher working voltages due to the higher potential of the metal-based cathode material as compared to ORR/OER at an air cathode, even though their theoretical capacities are lower. Therefore, when integrating both reaction mechanisms, hybrid Zn batteries could benefit from both a high operating voltage from the Zn-ion reaction and a superior capacity from the Zn-air reaction [155].

Similar to a Zn-ion battery, a hybrid Zn battery is composed of a Zn anode, an electrolyte, and a cathode that contains an active material. Yet, instead of employing a closed system, the cathode of a hybrid Zn battery is exposed to air, which provides oxygen access for the Zn-air reaction. In this way, the active reactant for the Zn-ion reaction could simultaneously function as an oxygen catalyst for the Zn-air reaction, thereby integrating the two battery systems without the need for extra components [156]. Thus, an ideal active material should possess a high cathodic potential for the Zn-ion reaction and also excellent catalytic activities for the ORR and OER.

As a result, transition metal compounds such as Ni-, Co-, and Ag-based oxides and sulfides gained tremendous attention as promising cathode materials for hybrid Zn batteries. Ni- and Co-based active materials typically exhibit higher OER activities but lower ORR activities and poorer electrical conductivity than Ag [155]. However, a recent study by Wang et. al. suggested the use of $NiCo_2S_4$ as active material, which possesses a much higher electrical conductivity than pure Ni or Co derivatives such as Co_3O_4 and NiO. Using $NiCo_2S_4$ nanotubes grown on 3D N-doped carbon as cathode, the resulting hybrid Zn battery is able to deliver a high working voltage of 1.75 V with a superior specific capacity of 626 $mAhg^{-1}$ [157].

Hybrid Zn batteries typically exhibit multiple discharge voltage plateaus corresponding to the distinctive Zn-ion and Zn-air reaction mechanisms. In the above study, the 1.75 V plateau originates from the Zn-$NiCo_2S_4$ reaction, while a subsequent plateau of 1.08 V corresponds to the

Zn-air reaction [157]. Another example is the Zn-Ag/ Zn-air hybrid battery developed by Tan et. al, which displays two-step voltage plateaus of 1.85 and 1.53 V as Ag undergoes two valence states

$$2AgO + H_2O + 2e^- \leftrightarrow Ag_2O + 2OH^- \quad (5a)$$

$$Ag_2O + H_2O + 2e^- \leftrightarrow 2Ag + 2OH^- \quad (5b)$$

(Equations 5a-b), then a 1.25 V plateau corresponding to the Zn-air reaction. At the same time, the hybrid battery delivers a high discharge capacity of 800 $mAhg^{-1}$ which exceeds that of a Zn-Ag battery alone [158]. Taking advantage of the higher voltage enabled by the Zn-ion reaction, hybrid Zn batteries exhibit a higher energy density and energy efficiency than conventional Zn-air batteries. Due to the high intrinsic electrical conductivity of Ag, the battery also benefits from a higher utilization ratio of catalytic material, leading to superior capacity.

Table 4 summarizes the recent developments of hybrid Zn batteries, showing the high operating voltages of 1.6-1.9 V and high energy efficiencies of 60-85% as they maintain remarkable discharge capacities and energy densities. Long operating lives of more than 1000 cycles were also achieved in many of these contributions, particularly in the Zn-$NiCo_2S_4$/ Zn-air hybrid battery developed by Li et. al., which delivered 5000 stable cycles over more than three months [159].

However, this recent trend in hybrid Zn batteries comes with its own hurdles. Although the working discharge voltages of the hybrid Zn batteries are higher than that of conventional Zn-air batteries, they are still largely hindered by the limitations of the cathode material, such as the poor utilization rate and insufficient catalytic activities. In order to achieve a breakthrough in the performance of hybrid Zn batteries, transition metal derivatives must be further explored and engineered through electronic tuning and structural alterations. The loading and material choice of the cathode must also be carefully optimized to balance its contribution in both the Zn-ion and Zn-air reactions. Furthermore, comprehensive characterizations are essential to evaluate the mechanisms of distinctive reaction stages during battery cycling, such that any unwanted parasitic reactions could be systematically addressed.

Table 4: Literature selection of hybrid Zn-ion/ Zn-air batteries published in the last 5 years

Hybrid system	Discharge voltage plateaus (V)	Discharge capacity ($mAhg^{-1}$)	Energy density ($Wh\ kg^{-1}$)	Discharge-charge voltage gap (V) @ current density[1]	Cycling stability @ current density[1]	Round trip efficiency	Ref.
Zn-$NiCo_2S_4$/ Zn-air	1.75, 1.08	626	688	0.75 (1 $mAcm^{-2}$)	400 cycles, 400 h (1 $mAcm^{-2}$)		[157]
Zn-$NiCo_2S_4$/ Zn-air	1.7, 1.0	688		1.0 (5 $mAcm^{-2}$)	5000 cycles, 2160 h (5 $mAcm^{-2}$)	60%	[159]
Zn-Ni/ Zn-air	1.7, 1.1			1.0 (20 $mAcm^{-2}$)	1100 h (20 $mAcm^{-2}$)	78%	[160]
Zn-Ag/ Zn-air	1.85, 1.53, 1.25	800	944	1.07 (10 $mAcm^{-2}$)	100 cycles (10 $mAcm^{-2}$)	68%	[158]
Zn-Ag/ Zn-air	1.8, 1.5, 1.1			1.0 (20 $mAcm^{-2}$)	1700 cycles, 551 h (20 $mAcm^{-2}$)	85%	[161]
Zn-Co_3O_{4-x}/ Zn-air	1.92, 1.1	800	1060	0.8 (5 $mAcm^{-2}$)	1500 cycles, 440 h (5 $mAcm^{-2}$)		[162]
Zn-Co_3O_4/ Zn-air	1.6, 1.05	771		1.2 (10 $mAcm^{-2}$)	1000 cycles, 333 h (10 $mAcm^{-2}$)	70%	[163]
Zn-Co_3O_4/ Zn-air	1.75, 1.11	711	810	0.8 (1 $mAcm^{-2}$)	600 cycles, 600 h (1 $mAcm^{-2}$)		[164]
Zn-$Co_{3-x}Ni_xO_4$/ Zn-air	1.67, 1.10	812	922	0.7 (5 $mAcm^{-2}$)	200 cycles, 200 h (5 $mAcm^{-2}$)	62%	[165]
Zn-Ni_3S_2/ Zn-air	1.7, 1.1		1105	1.0 (10 $mAcm^{-2}$)	300 h (10 $mAcm^{-2}$)		[166]
Zn-Ni-Co/COOH/ Zn-air	1.7, 1.0	146	945	1.0 (4 mA cm^{-2})	333 cycles, 100 h (4 mA cm^{-2})		[167]

[1] The discharge-charge voltage gap refers to the difference between the charge voltage and the discharge voltage plateaus during galvanostatic cycling. Some of the voltage data are derived from the figures when not reported in text by the authors.

4. Future Perspectives

Recent advancements have brought rechargeable Zn-air batteries closer to the market, but currently, most batteries could only cycle for a few hundred hours, with a round-trip energy efficiency of around 60-70%. In some cases, the power densities are insufficient, while the discharging and charging overpotentials are still significant. Besides, most of the reported batteries are cycled with a low depth-of-discharge only, which minimises material degradation and slows down capacity

fading in the cell [168]. Such condition unrealistically exaggerates both the reported cycle life and energy density, which fail to reflect the battery's practical operating performance. In order to replace Li-ion batteries as the power source for electric vehicles and consumer electronics, Zn-air batteries must reach superior long-term cyclic performances under practical operating conditions, which calls for further research and optimization. Some of the most promising research directions include alternative electrolytes, advanced catalysts, and hybrid Zn batteries, which have already enabled longer periods of stable cycling, up to a few thousand hours. Nevertheless, each strategy has its own limitations, for example compromising conductivity, adding complexity, and increasing costs. More importantly, the limited knowledge of the underlying mechanisms is a common problem across many of these recent advancements, which acts as the main bottleneck hindering new research breakthroughs.

First of all, a more rational design framework of bifunctional oxygen catalysts is strongly desired over trial-and-error iterations in the future. To this end, MOFs and single atom engineering are promising research directions that could pave the way for the systematic optimization of catalysts. Therefore, future studies should expand the limited understanding of the precise formation mechanisms behind MOFs to enable a more methodical tuning of catalyst materials. Upcoming research efforts should also focus on the stabilization of high-loading single atom catalysts, which is the main obstacle hindering their practical fabrication currently. It is also worth exploring other innovative design ideas, including photoactive catalysts that make use of solar energy, which could increase reaction kinetics and battery efficiency, especially for outdoor applications under sufficient sunlight [169].

The material optimization of bifunctional oxygen catalysts has dominated most of the latest research publications on Zn-air batteries. Thus, this perspective strongly encourages more research contributions on electrolyte development, which arguably exerts an even stronger impact on the fundamental mechanisms of a Zn-air battery. For example, neutral electrolytes could completely bypass the traditional alkaline-based parasitic reactions limiting the cycle life of Zn-air batteries. Since the battery's energy efficiency is strongly influenced by the parasitic reactions, electrolyte oxidation, and internal resistance in the battery cell, the development of advanced electrolytes plays a major role in generating a high-energy Zn-air battery. While studies on quasi-neutral electrolytes such as water-in-salt systems are growing, available literature is still scarce and their specific applications in Zn-air batteries are still limited. To advance their development, it is crucial

to gain an in-depth understanding of the anode reversibility mechanism and oxygen redox chemistries in the different types of electrolytes, including salts and ionic liquids containing different anion species. In the same way, studies on additive materials also suffer from the same problem of insufficient characterization information. To concurrently improve the performance of alkaline-based Zn-air batteries, it is essential to investigate the precise effects of each type of additive through thorough characterizations and analyses rather than blind experimentation.

In addition, future efforts in mathematical modelling and dynamic simulations could help expedite research progress in both the electrodes and electrolyte. By emphasizing the efficient screening of new materials and design strategies, modelling contributions could effectively eliminate unfavorable options without time-consuming trial-and-error experimentation. In turn, experimental investigations should provide abundant and accessible data to support and validate these models.

Next, it is worthwhile to mention that quasi-solid-state batteries have emerged as another promising future prospect of rechargeable Zn-air batteries, inspired by recent developments such as sponge-like electrodes and polymer gel electrolytes. Due to their high energy density, intrinsic safety, and long lifespan, solid-state batteries are considered the next-generation power source after traditional liquid batteries [170]. Apart from powering flexible wearable devices, solid-state batteries provide excellent prospects in electric vehicle applications. Toyota plans to unveil an electric vehicle prototype powered by solid-state batteries with an ultrafast charging time and 500 km driving range in 2021, while other car manufacturers and startups have also announced solid-state battery production goals by 2025 [171]. The development of quasi-solid-state Zn-air batteries is still at an early stage, and their performances are currently more suitable for low-power wearable devices, but they could hold great promise for future applications in the growing EV industry.

Finally, efficient battery fabrication plays a vital role in the future commercialization of Zn-air batteries. In recent years, advanced manufacturing techniques such as 3D printing and laser processing have emerged [172], giving rise to the development of 3D-printed porous electrodes [173] and paper-based Zn-air batteries [174], and opening up future possibilities for low-cost, scalable battery assembly. An interesting concept of hand-drawn printable batteries has also been proposed to facilitate customizable devices for on-demand fabrication [175]. However, to increase the prevalence of Zn-air batteries in EVs and grid-scale applications, the manufacturing process must be efficient and scalable while maintaining cost-competitiveness, which is a critical challenge

currently. Therefore, continuous research efforts in the electrode, electrolyte, and bifunctional oxygen catalyst are necessary with a strong emphasis in cost optimization and fabrication efficiency.

5. Summary and Outlook

Substantial progress has been made on the advancement of rechargeable Zn-air batteries in recent years. Structural modifications in the anode and the application of additives have successfully mitigated adverse water-induced reactions, while the use of polymer gels, flow battery system, and alternative electrolytes helped impede carbonate formation and water evaporation, prolonging the rechargeability of the Zn-air battery from a few hundred cycles to a few thousand cycles. Moreover, the material and engineering development of bifunctional oxygen catalysts at the air cathode have gained the most research attention, accelerating the electrochemical kinetics of the redox reactions, and achieving energy efficiencies up to 70%. These strategies have opened new avenues in advanced electrodes and electrolytes, inspired the development of solid-state batteries and hybrid Zn batteries, and paved the way for a more rational design of bifunctional oxygen catalysts.

However, the latest performances of Zn-air batteries are still inferior to state-of-the-art Li-ion batteries. Critical challenges remain, for example in the poor conductivity of polymer gel materials in solid-state electrolytes, and the high cost of ionic liquids. The uncertain battery mechanisms under quasi-neutral electrolytes, the difficult synthesis of high-loading single atom catalysts, and the added complexity in hybrid Zn batteries are other bottlenecks hindering their development. To enable the widespread adoption of rechargeable Zn-air batteries, future research directions should particularly focus on the systematic experimentation of alternative electrolytes, rational catalyst engineering, accurate mathematical modeling, and low-cost, efficient manufacturing. The demand for a safe, affordable, and high-performing rechargeable battery technology is surging in the energy and electronics industries. To meet this change, there is an urgent need to accelerate the research and development of rechargeable Zn-air batteries.

Acknowledgement:

This project is partially funded by the CRF of the Hong Kong Research Grant Council (C5031-20G).

References

1. Fu, J., et al., *Electrically rechargeable zinc–air batteries: progress, challenges, and perspectives.* Adv. Mater., 2017. **29**(7): p. 1604685.
2. Zhang, J., et al., *Zinc–air batteries: are they ready for prime time?* Chem. Sci., 2019. **10**(39): p. 8924-8929.
3. R. Mainar, A., et al., *Alkaline aqueous electrolytes for secondary zinc–air batteries: an overview.* Int. J. Energy Res., 2016. **40**(8): p. 1032-1049.
4. Blurton, K.F. and A.F. Sammells, *Metal/air batteries: their status and potential—a review.* J. Power Sources, 1979. **4**(4): p. 263-279.
5. Gu, P., et al., *Rechargeable zinc–air batteries: a promising way to green energy.* J. Mater. Chem. A, 2017. **5**(17): p. 7651-7666.
6. Lee, J.S., et al., *Metal–air batteries with high energy density: Li–air versus Zn–air.* Adv Energy Mater, 2011. **1**(1): p. 34-50.
7. Caramia, V. and B. Bozzini, *Materials science aspects of zinc–air batteries: a review.* Mater Renew Sustain Energy, 2014. **3**(2): p. 1-12.
8. Lee, S.-H., et al., *The stable rechargeability of secondary Zn-air batteries: is it possible to recharge a Zn-air battery?* J Korean Electrochem Soc, 2010. **13**(1): p. 45-49.
9. Gu, P., et al., *Rechargeable zinc–air batteries: a promising way to green energy.* J Mater Chem A, 2017. **5**(17): p. 7651-7666.
10. Prakoso, B., et al., *Recent Progress in Extending the Cycle‐Life of Secondary Zn‐Air Batteries.* ChemNanoMat, 2021. **7**(4): p. 354-367.
11. Wang, H.F., C. Tang, and Q. Zhang, *A review of precious‐metal‐free bifunctional oxygen electrocatalysts: rational design and applications in Zn− air batteries.* Adv Funct Mater, 2018. **28**(46): p. 1803329.
12. Cai, X., et al., *Recent advances in air electrodes for Zn–air batteries: electrocatalysis and structural design.* Mater Horiz, 2017. **4**(6): p. 945-976.
13. Chen, P., et al., *Recent Progress in Electrolytes for Zn–Air Batteries.* Front Chem, 2020. **8**.
14. Zhou, T., et al., *Surface/interface nanoengineering for rechargeable Zn–air batteries.* Energy Environ Sci, 2020. **13**(4): p. 1132-1153.
15. Davari, E. and D. Ivey, *Bifunctional electrocatalysts for Zn–air batteries.* Sustain Energy Fuels, 2018. **2**(1): p. 39-67.
16. NantEnergy. *Zinc-air storage: Rugged, long-duration, pollution-free energy storage systems for use in any location*. 2019 2019; Available from: https://nantenergy.com/zinc-air/.
17. Khan, P.A. and B. Venkatesh, *Economic Analysis of Chemical Energy Storage Technologies*, in *Smart City 360°*. 2016, Springer. p. 277-291.
18. Fu, J., et al., *Recent progress in electrically rechargeable zinc–air batteries.* Adv. Mater., 2019. **31**(31): p. 1805230.
19. Kim, H.-I., et al., *Influence of ZnO precipitation on the cycling stability of rechargeable Zn–air batteries.* J. Appl. Electrochem., 2015. **45**(4): p. 335-342.
20. Parker, J.F., et al., *Wiring zinc in three dimensions re-writes battery performance—dendrite-free cycling.* Energy Environ. Sci., 2014. **7**(3): p. 1117-1124.
21. Zhang, X.G., *Corrosion and electrochemistry of zinc*. 1996: Springer Science & Business Media.

22. Zhao, Z., et al., *Challenges in zinc electrodes for alkaline zinc–air batteries: obstacles to commercialization.* ACS Energy Lett., 2019. **4**(9): p. 2259-2270.
23. Einerhand, R., W. Visscher, and E. Barendrecht, *Hydrogen production during zinc deposition from alkaline zincate solutions.* J. Appl. Electrochem., 1988. **18**(6): p. 799-806.
24. Dobryszycki, J. and S. Biallozor, *On some organic inhibitors of zinc corrosion in alkaline media.* Corros. Sci., 2001. **43**(7): p. 1309-1319.
25. Li, Y., et al., *The role of PTFE in cathode transition layer in aqueous electrolyte Li-air battery.* Electrochim. Acta, 2016. **191**: p. 996-1000.
26. Xu, M., et al., *Rechargeable Zn-air batteries: Progress in electrolyte development and cell configuration advancement.* J. Power Sources, 2015. **283**: p. 358-371.
27. Chen, P., et al., *Recent Progress in Electrolytes for Zn–Air Batteries.* Front. Chem., 2020. **8**.
28. Li, Y. and H. Dai, *Recent advances in zinc–air batteries.* Chem. Soc. Rev., 2014. **43**(15): p. 5257-5275.
29. Yano, M., et al., *Effect of additives in zinc alloy powder on suppressing hydrogen evolution.* J. Power Sources, 1998. **74**(1): p. 129-134.
30. Jo, Y.N., et al., *The effects of mechanical alloying on the self-discharge and corrosion behavior in Zn-air batteries.* J. Ind. Eng. Chem., 2017. **53**: p. 247-252.
31. Chotipanich, J., et al., *Electronic and ionic conductivities enhancement of zinc anode for flexible printed zinc-air battery.* Eng. J., 2018. **22**(2): p. 47-57.
32. Park, D.-J., E.O. Aremu, and K.-S.J.A.S.S. Ryu, *Bismuth oxide as an excellent anode additive for inhibiting dendrite formation in zinc-air secondary batteries.* 2018. **456**: p. 507-514.
33. Aremu, E.O., D.-J. Park, and K.-S. Ryu, *The effects of anode additives towards suppressing dendrite growth and hydrogen gas evolution reaction in Zn-air secondary batteries.* Ionics, 2019. **25**(9): p. 4197-4207.
34. Lee, S.-M., et al., *Improvement in self-discharge of Zn anode by applying surface modification for Zn–air batteries with high energy density.* 2013. **227**: p. 177-184.
35. Zhao, K., et al., *Ultrathin surface coating enables stabilized zinc metal anode.* 2018. **5**(16): p. 1800848.
36. Kim, Y.-J. and K.-S.J.A.S.S. Ryu, *The surface-modified effects of Zn anode with CuO in Zn-air batteries.* 2019. **480**: p. 912-922.
37. Zhang, Y., et al., *Sealing ZnO nanorods for deeply rechargeable high-energy aqueous battery anodes.* Nano Energy, 2018. **53**: p. 666-674.
38. Schmid, M. and M. Willert-Porada, *Electrochemical behavior of zinc particles with silica based coatings as anode material for zinc air batteries with improved discharge capacity.* J. Power Sources, 2017. **351**: p. 115-122.
39. Jo, Y.N., et al., *Improving self-discharge and anti-corrosion performance of Zn-air batteries using conductive polymer-coated Zn active materials.* J. Ind. Eng. Chem., 2019. **76**: p. 396-402.
40. Hoang, T.K., K.E.K. Sun, and P.J.R.A. Chen, *Corrosion chemistry and protection of zinc & zinc alloys by polymer-containing materials for potential use in rechargeable aqueous batteries.* 2015. **5**(52): p. 41677-41691.
41. Lee, C.W., et al., *Effect of additives on the electrochemical behaviour of zinc anodes for zinc/air fuel cells.* 2006. **160**(1): p. 161-164.

42. Zhang, Z., et al., *Preparation and properties of ZnO/PVA/β-CD/PEG composite electrode for rechargeable zinc anode.* J. Electroanal. Chem., 2018. **827**: p. 85-92.
43. Lin, H., C. Ho, and C. Lee, *Discharge performance of zinc coating prepared by pulse electroplating with different frequencies for application in zinc-air battery.* Surf. Coat. Technol., 2017. **319**: p. 378-385.
44. Tan, W.K., et al., *Fabrication of an all-solid-state Zn-air battery using electroplated Zn on carbon paper and KOH-ZrO2 solid electrolyte.* Appl. Surf. Sci., 2019. **487**: p. 343-348.
45. Pan, Z., et al., *All-solid-state sponge-like squeezable zinc-air battery.* Energy Storage Mater., 2019. **23**: p. 375-382.
46. Kim, Y.-J. and K.-S. Ryu, *The surface-modified effects of Zn anode with CuO in Zn-air batteries.* Appl. Surf. Sci., 2019. **480**: p. 912-922.
47. Wei, H., et al., *Zn@ C Core–Shell Nanocomposite for Rechargeable Aqueous Zn//MnO2 Batteries with Long Lifetime.* Energy Technol., 2019. **7**(4): p. 1800912.
48. Liu, P., et al., *Porous zinc anode design for zn-air chemistry.* Front. Chem., 2019. **7**: p. 656.
49. Qu, S., et al., *Kirigami-Inspired Flexible and Stretchable Zinc–Air Battery Based on Metal-Coated Sponge Electrodes.* ACS Appl. Mater. Interfaces, 2020.
50. Huang, M.C., et al., *Improved electrochemical performance of Zn–air secondary batteries via novel organic additives.* J. Chin. Chem. Soc., 2018. **65**(10): p. 1239-1244.
51. Banik, S.J. and R.J.J.o.T.E.S. Akolkar, *Suppressing dendrite growth during zinc electrodeposition by PEG-200 additive.* 2013. **160**(11): p. D519.
52. Sun, K.E., et al., *Suppression of dendrite formation and corrosion on zinc anode of secondary aqueous batteries.* 2017. **9**(11): p. 9681-9687.
53. Miyazaki, K., et al., *Influence of surfactants as additives to electrolyte solutions on zinc electrodeposition and potential oscillation behavior.* J Appl Electrochem, 2016. **46**(10): p. 1067-1073.
54. Hosseini, S., et al., *Discharge performance of zinc-air flow batteries under the effects of sodium dodecyl sulfate and pluronic F-127.* Sci. Rep., 2018. **8**(1): p. 1-13.
55. Khezri, R., et al., *Enhanced Cycling Performance of Rechargeable Zinc–Air Flow Batteries Using Potassium Persulfate as Electrolyte Additive.* Int. J. Mol. Sci., 2020. **21**(19): p. 7303.
56. Hosseini, S., et al., *Ethanol as an electrolyte additive for alkaline zinc-air flow batteries.* Sci. Rep., 2018. **8**(1): p. 1-11.
57. Hosseini, S., et al., *The influence of dimethyl sulfoxide as electrolyte additive on anodic dissolution of alkaline zinc-air flow battery.* Sci. Rep., 2019. **9**(1): p. 1-12.
58. Abbasi, A., et al., *Discharge profile of a zinc-air flow battery at various electrolyte flow rates and discharge currents.* Sci. Data, 2020. **7**(1): p. 1-8.
59. Ma, L., et al., *Super‐Stretchable Zinc‐Air Batteries Based on an Alkaline‐Tolerant Dual‐Network Hydrogel Electrolyte.* Adv. Energy Mater., 2019. **9**(12): p. 1803046.
60. Song, Z., et al., *A Rechargeable Zn‐Air Battery with High Energy Efficiency and Long Life Enabled by a Highly Water‐Retentive Gel Electrolyte with Reaction Modifier.* Adv. Mater., 2020. **32**(22): p. 1908127.
61. Huang, Y., et al., *Solid‐State Rechargeable Zn//NiCo and Zn‐Air Batteries with Ultralong Lifetime and High Capacity: The Role of a Sodium Polyacrylate Hydrogel Electrolyte.* Adv. Energy Mater., 2018. **8**(31): p. 1802288.

62. Mainar, A.R., et al., *An overview of progress in electrolytes for secondary zinc-air batteries and other storage systems based on zinc.* J. Energy Storage, 2018. **15**: p. 304-328.
63. Mainar, A.R., et al., *An overview of progress in electrolytes for secondary zinc-air batteries and other storage systems based on zinc.* 2018. **15**: p. 304-328.
64. Yu, N.-F., et al., *Highly efficient Co3O4/Co@ NCs bifunctional oxygen electrocatalysts for long life rechargeable Zn-air batteries.* 2020. **77**: p. 105200.
65. Kar, M. and C. Pozo-Gonzalo, *Emergence of non-aqueous electrolytes for rechargeable zinc batteries.* Curr. Opin. Green Sustain., 2020: p. 100426.
66. Wang, F., et al., *Highly reversible zinc metal anode for aqueous batteries.* Nat. Mater., 2018. **17**(6): p. 543-549.
67. Sun, W., et al., *A rechargeable zinc-air battery based on zinc peroxide chemistry.* Science, 2021. **371**(6524): p. 46-51.
68. Singh, H., et al., *Carbon-based catalysts for oxygen reduction reaction: A review on degradation mechanisms.* Carbon, 2019. **151**: p. 160-174.
69. Liu, S., et al., *A novel rechargeable zinc-air battery with molten salt electrolyte.* J. Power Sources, 2017. **342**: p. 435-441.
70. Ingale, P., M. Sakthivel, and J.-F. Drillet, *Test of diethylmethylammonium trifluoromethanesulfonate ionic liquid as electrolyte in electrically rechargeable Zn/Air battery.* J. Electrochem. Soc., 2017. **164**(8): p. H5224.
71. Alwast, D., et al., *Ionic Liquid Electrolytes for Metal-Air Batteries: Interactions between O2, Zn2+ and H2O Impurities.* J. Electrochem. Soc., 2019. **167**(7): p. 070505.
72. Kar, M., et al., *Ionic liquid electrolytes as a platform for rechargeable metal–air batteries: a perspective.* Phys. Chem. Chem. Phys., 2014. **16**(35): p. 18658-18674.
73. Sumboja, A., et al., *Durable rechargeable zinc-air batteries with neutral electrolyte and manganese oxide catalyst.* Journal of Power Sources, 2016. **332**: p. 330-336.
74. Li, M., et al., *Long-shelf-life polymer electrolyte based on tetraethylammonium hydroxide for flexible zinc–air batteries.* ACS Appl. Mater. Interfaces, 2019. **11**(32): p. 28909-28917.
75. Fan, X., et al., *Porous nanocomposite gel polymer electrolyte with high ionic conductivity and superior electrolyte retention capability for long-cycle-life flexible zinc–air batteries.* Nano Energy, 2019. **56**: p. 454-462.
76. Miao, H., et al., *All-solid-state flexible zinc-air battery with polyacrylamide alkaline gel electrolyte.* J. Power Sources, 2020. **450**: p. 227653.
77. Pei, Z., et al., *Enabling highly efficient, flexible and rechargeable quasi-solid-state zn-air batteries via catalyst engineering and electrolyte functionalization.* Energy Storage Materials, 2019. **20**: p. 234-242.
78. Chen, C.Y., et al., *A room‐temperature molten hydrate electrolyte for rechargeable zinc–air batteries.* 2019. **9**(22): p. 1900196.
79. Fu, G., Y. Tang, and J.M.J.C. Lee, *Recent Advances in Carbon‐Based Bifunctional Oxygen Electrocatalysts for Zn− Air Batteries.* 2018. **5**(11): p. 1424-1434.
80. Tomboc, G.M., et al., *Ideal design of air electrode—A step closer toward robust rechargeable Zn–air battery.* APL Mater., 2020. **8**(5): p. 050905.
81. Fang, G., et al., *Multi-component nanoporous alloy/(oxy) hydroxide for bifunctional oxygen electrocatalysis and rechargeable Zn-air batteries.* Appl. Catal. B, 2020. **268**: p. 118431.

82. Tian, Y., et al., *Rational design of sustainable transition metal-based bifunctional electrocatalysts for oxygen reduction and evolution reactions.* Sustainable Mater. Technol., 2020: p. e00204.
83. Wu, M., et al., *Rational design of multifunctional air electrodes for rechargeable Zn–Air batteries: Recent progress and future perspectives.* Energy Storage Mater., 2019. **21**: p. 253-286.
84. Lang, X., Z. Hu, and C. Wang, *Bifunctional air electrodes for flexible rechargeable Zn-air batteries.* Chin. Chem. Lett., 2020.
85. Dai, Y., et al., *Rational design of spinel oxides as bifunctional oxygen electrocatalysts for rechargeable Zn-air batteries.* Chemical Physics Reviews, 2020. **1**(1): p. 011303.
86. Yu, X., et al., *Recent advances on the modulation of electrocatalysts based on transition metal nitrides for the rechargeable Zn-air battery.* ACS Mater. Lett., 2020. **2**(11): p. 1423-1434.
87. Dutta, A. and N. Pradhan, *Developments of metal phosphides as efficient OER precatalysts.* J. Phys. Chem. Lett., 2017. **8**(1): p. 144-152.
88. Sun, H., et al., *Self‐supported transition‐metal‐based electrocatalysts for hydrogen and oxygen evolution.* Adv. Mater., 2020. **32**(3): p. 1806326.
89. Liang, Y., et al., *Strongly coupled inorganic/nanocarbon hybrid materials for advanced electrocatalysis.* J. Am. Chem. Soc., 2013. **135**(6): p. 2013-2036.
90. Zhu, Y.P., et al., *Surface and interface engineering of noble-metal-free electrocatalysts for efficient energy conversion processes.* Acc. Chem. Res., 2017. **50**(4): p. 915-923.
91. Hu, C., et al., *Carbon‐based metal‐free catalysts for energy storage and environmental remediation.* Adv. Mater., 2019. **31**(13): p. 1806128.
92. Wang, Z., et al., *State-of-the-art on the production and application of carbon nanomaterials from biomass.* Green Chem., 2018. **20**(22): p. 5031-5057.
93. Marsudi, M.A., et al., *Manganese Oxide Nanorods Decorated Table Sugar Derived Carbon as Efficient Bifunctional Catalyst in Rechargeable Zn-Air Batteries.* Catalysts, 2020. **10**(1): p. 64.
94. Wu, Y.-j., et al., *Controlled synthesis of FeNx-CoNx dual active sites interfaced with metallic Co nanoparticles as bifunctional oxygen electrocatalysts for rechargeable Zn-air batteries.* Appl. Catal. B, 2020. **278**: p. 119259.
95. Wang, X., et al., *Electronic and Structural Engineering of Carbon‐Based Metal‐Free Electrocatalysts for Water Splitting.* Adv. Mater., 2019. **31**(13): p. 1803625.
96. Xiao, X., et al., *Anchoring NiCo2O4 nanowhiskers in biomass-derived porous carbon as superior oxygen electrocatalyst for rechargeable Zn-air battery.* J. Power Sources, 2020. **476**: p. 228684.
97. Luo, H., et al., *Self‐Catalyzed Growth of Co‐N‐C Nanobrushes for Efficient Rechargeable Zn‐Air Batteries.* Small, 2020. **16**(20): p. 2001171.
98. Chen, D., H. Feng, and J. Li, *Graphene oxide: preparation, functionalization, and electrochemical applications.* Chem. Rev., 2012. **112**(11): p. 6027-6053.
99. Xu, N., et al., *High-performing rechargeable/flexible zinc-air batteries by coordinated hierarchical Bi-metallic electrocatalyst and heterostructure anion exchange membrane.* Nano Energy, 2019. **65**: p. 104021.
100. Wu, Z., et al., *Molecularly Thin Nitride Sheets Stabilized by Titanium Carbide as Efficient Bifunctional Electrocatalysts for Fiber-Shaped Rechargeable Zinc-Air Batteries.* Nano Lett., 2020. **20**(4): p. 2892-2898.

101. Song, S., et al., *TiC supported amorphous MnOx as highly efficient bifunctional electrocatalyst for corrosion resistant oxygen electrode of Zn-air batteries.* Nano Energy, 2020. **67**: p. 104208.
102. Li, Y., et al., *Supramolecular assisted one-pot synthesis of donut-shaped CoP@ PNC hybrid nanostructures as multifunctional electrocatalysts for rechargeable Zn-air batteries and self-powered hydrogen production.* Energy Storage Mater, 2020. **28**: p. 27-36.
103. Yan, Y., et al., *Bifunctional nickel ferrite-decorated carbon nanotube arrays as free-standing air electrode for rechargeable Zn–air batteries.* J. Mater. Chem. A, 2020. **8**(10): p. 5070-5077.
104. Lu, X.F., et al., *Nitrogen‐Doped Cobalt Pyrite Yolk–Shell Hollow Spheres for Long‐Life Rechargeable Zn–Air Batteries.* Adv. Sci., 2020. **7**(22): p. 2001178.
105. Xiao, X., et al., *Robust template-activator cooperated pyrolysis enabling hierarchically porous honeycombed defective carbon as highly-efficient metal-free bifunctional electrocatalyst for Zn-air batteries.* Appl. Catal. B, 2020. **265**: p. 118603.
106. Tang, C., et al., *Defect engineering toward atomic Co–Nx–C in hierarchical graphene for rechargeable flexible solid Zn-air batteries.* Adv. Mater., 2017. **29**(37): p. 1703185.
107. Tang, C. and Q. Zhang, *Nanocarbon for oxygen reduction electrocatalysis: dopants, edges, and defects.* Adv. Mater., 2017. **29**(13): p. 1604103.
108. Li, F., et al., *Graphene oxide: A promising nanomaterial for energy and environmental applications.* Nano Energy, 2015. **16**: p. 488-515.
109. Shu, X., et al., *Cobalt nitride embedded holey N-doped graphene as advanced bifunctional electrocatalysts for Zn-Air batteries and overall water splitting.* Carbon, 2020. **157**: p. 234-243.
110. Zhou, T., et al., *Surface/interface nanoengineering for rechargeable Zn–air batteries.* Energy Environ. Sci., 2020. **13**(4): p. 1132-1153.
111. Li, M., et al., *Atomic layer Co3O4-x nanosheets as efficient and stable electrocatalyst for rechargeable zinc-air batteries.* J. Catal., 2020. **381**: p. 395-401.
112. Lyu, D., et al., *In situ molecular-level synthesis of N, S co-doped carbon as efficient metal-free oxygen redox electrocatalysts for rechargeable Zn–Air batteries.* Appl. Mater. Today, 2020. **20**: p. 100737.
113. Zhong, Y., et al., *Recent advances in metal-organic framework derivatives as oxygen catalysts for zinc-air batteries.* Batteries Supercaps, 2019. **2**(4): p. 272-289.
114. Zhou, Q., et al., *Template-guided synthesis of Co nanoparticles embedded in hollow nitrogen doped carbon tubes as a highly efficient catalyst for rechargeable Zn-air batteries.* Nano Energy, 2020. **71**: p. 104592.
115. Zhang, M., et al., *Novel MOF-derived Co@ N-C bifunctional catalysts for highly efficient Zn–air batteries and water splitting.* Adv. Mater., 2018. **30**(10): p. 1705431.
116. Xu, Y., et al., *2D Nitrogen-Doped Carbon Nanotubes/Graphene Hybrid as Bifunctional Oxygen Electrocatalyst for Long-Life Rechargeable Zn–Air Batteries.* Adv. Funct. Mater., 2020. **30**(6): p. 1906081.
117. Chen, Z., et al., *Recent advances in transition metal-based electrocatalysts for alkaline hydrogen evolution.* J. Mater. Chem. A, 2019. **7**(25): p. 14971-15005.

118. Mitchell, S., E. Vorobyeva, and J. Pérez‐Ramírez, *The multifaceted reactivity of single‐atom heterogeneous catalysts.* Angew. Chem. Int. Ed., 2018. **57**(47): p. 15316-15329.
119. Han, X., et al., *Generation of Nanoparticle, Atomic‐Cluster, and Single‐Atom Cobalt Catalysts from Zeolitic Imidazole Frameworks by Spatial Isolation and Their Use in Zinc–Air Batteries.* Angew. Chem., 2019. **131**(16): p. 5413-5418.
120. Sun, H., et al., *Updating the Intrinsic Activity of a Single-Atom Site with a P–O Bond for a Rechargeable Zn–Air Battery.* ACS Appl. Mater. Interfaces, 2019. **11**(36): p. 33054-33061.
121. Lang, R., et al., *Non defect-stabilized thermally stable single-atom catalyst.* Nat. Commun., 2019. **10**(1): p. 1-10.
122. Zhou, Y., et al., *Multilayer stabilization for fabricating high-loading single-atom catalysts.* Nat. Commun., 2020. **11**(1): p. 1-11.
123. Li, Z., et al., *Deep-Breathing Honeycomb-like Co-Nx-C Nanopolyhedron Bifunctional Oxygen Electrocatalysts for Rechargeable Zn-Air Batteries.* Iscience, 2020. **23**(8): p. 101404.
124. Sarawutanukul, S., et al., *Rechargeable Photoactive Zn‐air batteries Using NiCo2S4 as an Efficient Bifunctional Photocatalyst towards OER/ORR at the Cathode.* Batteries Supercaps, 2020. **3**(6).
125. Liu, P., et al., *Bifunctional Oxygen Electrocatalyst of Mesoporous Ni/NiO Nanosheets for Flexible Rechargeable Zn–Air Batteries.* Nano-Micro Lett., 2020. **12**(1): p. 1-12.
126. Li, M., et al., *Atomic layer Co3O4-x nanosheets as efficient and stable electrocatalyst for rechargeable zinc-air batteries.* Journal of Catalysis, 2020. **381**: p. 395-401.
127. Zhu, P., et al., *An efficient metal-free bifunctional oxygen electrocatalyst of carbon co-doped with fluorine and nitrogen atoms for rechargeable Zn-air battery.* Int. J. Hydrogen Energy, 2020. **45**(16): p. 9512-9521.
128. Zhang, D., et al., *Enhanced oxygen reduction and evolution in N-doped carbon anchored with Co nanoparticles for rechargeable Zn-air batteries.* Appl. Surf. Sci., 2020: p. 148700.
129. Hao, R., et al., *N-doped porous carbon hollow microspheres encapsulated with iron-based nanocomposites as advanced bifunctional catalysts for rechargeable Zn-air battery.* J. Energy Chem., 2020. **49**: p. 14-21.
130. Wang, J., et al., *Developing Indium-based Ternary Spinel Selenides for Efficient Solid Flexible Zn-Air Batteries and Water Splitting.* ACS Appl. Mater. Interfaces, 2020. **12**(7): p. 8115-8123.
131. Yang, Z., et al., *Encapsulated CoxSy nanoparticles decorated S, N-doped mesoporous carbon as effective bifunctional oxygen electrocatalyst in rechargeable Zn-air battery.* J. Alloys Compd., 2020: p. 157665.
132. Ren, J.-T., et al., *Binary FeNi phosphides dispersed on N, P-doped carbon nanosheets for highly efficient overall water splitting and rechargeable Zn-air batteries.* Chem. Eng. J., 2020. **389**: p. 124408.
133. Chandrappa, S.G., et al., *The influence of ruthenium substitution in LaCoO 3 towards bi-functional electrocatalytic activity for rechargeable Zn–air batteries.* J. Mater. Chem. A, 2020. **8**(39): p. 20612-20620.

134. Majee, R., et al., *Shaping a Doped Perovskite Oxide with Measured Grain Boundary Defects to Catalyze Bifunctional Oxygen Activation for a Rechargeable Zn–Air Battery.* ACS Appl. Mater. Interfaces, 2020. **12**(36): p. 40355-40363.
135. Wu, Y.-j., et al., *Controlled synthesis of FeNx-CoNx dual active sites interfaced with metallic Co nanoparticles as bifunctional oxygen electrocatalysts for rechargeable Zn-air batteries.* Applied Catalysis B: Environmental, 2020. **278**: p. 119259.
136. Sun, X., et al., *Exploiting a High-Performance "Double-Carbon" Structure Co9S8/GN Bifunctional Catalysts for Rechargeable Zn–Air Batteries.* ACS Appl. Mater. Interfaces, 2020. **12**(34): p. 38202-38210.
137. Wang, Y., et al., *In situ growth of CoP nanoparticles anchored on (N, P) co-doped porous carbon engineered by MOFs as advanced bifunctional oxygen catalyst for rechargeable Zn–air battery.* J. Mater. Chem. A, 2020. **8**(36): p. 19043-19049.
138. Wu, Z., et al., *Sulfurated Metal-Organic Frameworks Derived Nanocomposites for Efficient Bifunctional Oxygen Electrocatalysis and Rechargeable Zn-air Battery.* ACS Sustainable Chem. Eng., 2020. **8**(24).
139. Guo, X., et al., *Synthesis of confining cobalt nanoparticles within SiOx/nitrogen-doped carbon framework derived from sustainable bamboo leaves as oxygen electrocatalysts for rechargeable Zn-air batteries.* Chem. Eng. J., 2020. **401**: p. 126005.
140. Zhang, H.-M., et al., *Co/Co 9 S 8@ carbon nanotubes on a carbon sheet: facile controlled synthesis, and application to electrocatalysis in oxygen reduction/oxygen evolution reactions, and to a rechargeable Zn-air battery.* Inorg. Chem. Front., 2020.
141. Arafat, Y., et al., *A Porous Nano-Micro-Composite as a High-Performance Bi-Functional Air Electrode with Remarkable Stability for Rechargeable Zinc–Air Batteries.* Nano-Micro Lett., 2020. **12**(1): p. 1-16.
142. Wang, X., et al., *High-performance metal-organic framework-perovskite hybrid as an important component of the air-electrode for rechargeable Zn-Air battery.* J. Power Sources, 2020. **468**: p. 228377.
143. Niu, Y., et al., *A" trimurti" heterostructured hybrid with an intimate CoO/Co x P interface as a robust bifunctional air electrode for rechargeable Zn–air batteries.* J. Mater. Chem. A, 2020. **8**(18): p. 9177-9184.
144. Lai, C., et al., *Bimetallic organic framework-derived rich pyridinic N-doped carbon nanotubes as oxygen catalysts for rechargeable Zn-air batteries.* J. Power Sources, 2020. **472**: p. 228470.
145. Tan, J., et al., *Rapid microwave-assisted preparation of high-performance bifunctional Ni3Fe/Co-NC for rechargeable Zn-air battery.* Chem. Eng. J., 2020: p. 125151.
146. Chen, D., et al., *Hierarchical architecture derived from two-dimensional zeolitic imidazolate frameworks as an efficient metal-based bifunctional oxygen electrocatalyst for rechargeable Zn–air batteries.* Electrochim. Acta, 2020. **331**: p. 135394.
147. Yu, N.-F., et al., *Highly efficient Co3O4/Co@ NCs bifunctional oxygen electrocatalysts for long life rechargeable Zn-air batteries.* Nano Energy, 2020. **77**: p. 105200.
148. Chen, G., et al., *Continuous nitrogen-doped carbon nanotube matrix for boosting oxygen electrocatalysis in rechargeable Zn-air batteries.* J Energy Chem, 2021. **55**: p. 183-189.
149. Jose, V., et al., *Modulation of Single Atomic Co and Fe Sites on Hollow Carbon Nanospheres as Oxygen Electrodes for Rechargeable Zn–Air Batteries.* Small Methods, 2020: p. 2000751.

150. Qin, T., et al., *Ionic Liquid Derived Active Atomic Iron Sites Anchored on Hollow Carbon Nanospheres for Bifunctional Oxygen Electrocatalysis.* Chem. Eng. J., 2020: p. 125656.
151. Zhong, X., et al., *Co single-atom anchored on Co3O4 and nitrogen-doped active carbon toward bifunctional catalyst for zinc-air batteries.* Appl. Catal. B, 2020. **260**: p. 118188.
152. Li, B.Q., et al., *Framework‐porphyrin‐derived single‐atom bifunctional oxygen electrocatalysts and their applications in Zn‐air batteries.* Adv. Mater., 2019. **31**(19): p. 1900592.
153. Xiao, M., et al., *Preferentially Engineering FeN4 Edge Sites onto Graphitic Nanosheets for Highly Active and Durable Oxygen Electrocatalysis in Rechargeable Zn–Air Batteries.* Adv. Mater., 2020. **32**(49): p. 2004900.
154. Zang, W., et al., *Single Co atoms anchored in porous N-doped carbon for efficient zinc–air battery cathodes.* ACS Catalysis, 2018. **8**(10): p. 8961-8969.
155. Shang, W., et al., *Achieving high energy density and efficiency through integration: progress in hybrid zinc batteries.* J Mater Chem A, 2019. **7**(26): p. 15564-15574.
156. Lee, D.U., et al., *Self-assembled NiO/Ni (OH) 2 nanoflakes as active material for high-power and high-energy hybrid rechargeable battery.* Nano letters, 2016. **16**(3): p. 1794-1802.
157. Wang, X., et al., *Combination of Zn–NiCo2S4 and Zn–Air Batteries at the Cell Level: A Hybrid Battery Makes the Best of Both Worlds.* ACS Sustainable Chem Eng, 2019. **7**(14): p. 12331-12339.
158. Tan, P., et al., *Integration of Zn–Ag and Zn–Air batteries: a hybrid battery with the advantages of both.* ACS Appl Mater Interfaces, 2018. **10**(43): p. 36873-36881.
159. Li, B., et al., *A robust hybrid Zn-battery with ultralong cycle life.* Nano Letters, 2017. **17**(1): p. 156-163.
160. Cheng, Y., et al., *A long-life hybrid zinc flow battery achieved by dual redox couples at cathode.* Nano Energy, 2019. **63**: p. 103822.
161. Chang, C.-C., et al., *Flexible Hybrid Zn–Ag/Air Battery with Long Cycle Life.* ACS Sustainable Chem Eng, 2018. **7**(2): p. 2860-2866.
162. Ma, L., et al., *Flexible waterproof rechargeable hybrid zinc batteries initiated by multifunctional oxygen vacancies-rich cobalt oxide.* ACS Nano, 2018. **12**(8): p. 8597-8605.
163. Tan, P., et al., *In-situ growth of Co3O4 nanowire-assembled clusters on nickel foam for aqueous rechargeable Zn-Co3O4 and Zn-air batteries.* Appl Catal B: Environ, 2019. **241**: p. 104-112.
164. Liu, H., et al., *A Co-MOF-derived oxygen-vacancy-rich Co 3 O 4-based composite as a cathode material for hybrid Zn batteries.* Dalton Transactions, 2020. **49**(9): p. 2880-2887.
165. Wu, M., et al., *A self-supported electrode as a high-performance binder-and carbon-free cathode for rechargeable hybrid zinc batteries.* Energy Storage Mater, 2020. **24**: p. 272-280.
166. Huang, Z., et al., *Ni 3 S 2/Ni nanosheet arrays for high-performance flexible zinc hybrid batteries with evident two-stage charge and discharge processes.* J Mater Chem A, 2019. **7**(32): p. 18915-18924.
167. Cui, M., et al., *Electrochemically induced NiCoSe2@ NiOOH/CoOOH heterostructures as multifunctional cathode materials for flexible hybrid zn batteries.* Energy Storage Materials, 2021. **36**: p. 427-434.

168. Watanabe, S., et al., *Capacity fading of LiAlyNi1− x− yCoxO2 cathode for lithium-ion batteries during accelerated calendar and cycle life tests (effect of depth of discharge in charge–discharge cycling on the suppression of the micro-crack generation of LiAlyNi1− x− yCoxO2 particle).* Journal of Power Sources, 2014. **260**: p. 50-56.
169. Liu, X., et al., *Utilizing solar energy to improve the oxygen evolution reaction kinetics in zinc–air battery.* Nat. Commun., 2019. **10**(1): p. 1-10.
170. Hu, Y.-S., *Batteries: getting solid.* Nat. Energy, 2016. **1**(4): p. 1-2.
171. NikkeiAsia, *Toyota's game-changing solid-state battery en route for 2021 debut.* 2020.
172. Wang, C., et al., *Recent progress of metal–air batteries—a mini review.* Appl. Sci., 2019. **9**(14): p. 2787.
173. Zhang, J., et al., *3D-printed functional electrodes towards Zn-Air batteries.* Materials Today Energy, 2020. **16**: p. 100407.
174. Ma, T. and J.D. MacKenzie, *Fully printed, high energy density flexible zinc-air batteries based on solid polymer electrolytes and a hierarchical catalyst current collector.* Flexible Printed Electron., 2019. **4**(1): p. 015010.
175. Choi, K.H., et al., *All‐Hand‐Drawn Zn–Air Batteries: Toward User‐Customized On‐the‐Fly Power Sources.* Adv. Sustainable Syst., 2018. **2**(5): p. 1700132.